FLORE
Repository istituzionale dell'Università degli Studi di Firenze

Visual impairment in FOXG1-mutated individuals and mice

Questa è la Versione finale referata (Post print/Accepted manuscript) della seguente pubblicazione:

Original Citation:

Visual impairment in FOXG1-mutated individuals and mice / Boggio, E.M.; Pancrazi, L.; Gennaro, M.; Lo Rizzo, C.; Mari, F.; Meloni, I.; Ariani, F.; Panighini, A.; Novelli, E.; Biagioni, M.; Strettoi, E.; Hayek, J.; Rufa, A.; Pizzorusso, T.; Renieri, A.; Costa, M.. - In: NEUROSCIENCE. - ISSN 0306-4522. - STAMPA. - 324(2016), pp. 496-508. [10.1016/j.neuroscience.2016.03.027]

Availability:

This version is available at: 2158/1087331 since: 2017-05-30T11:40:35Z

Published version:

DOI: 10.1016/j.neuroscience.2016.03.027

Terms of use:

Open Access

La pubblicazione è resa disponibile sotto le norme e i termini della licenza di deposito, secondo quanto stabilito dalla Policy per l'accesso aperto dell'Università degli Studi di Firenze (https://www.sba.unifi.it/upload/policy-oa-2016-1.pdf)

Publisher copyright claim:

(Article begins on next page)

20 December 2021

Elsevier Editorial System(tm) for Neuroscience

Manuscript Draft

Manuscript Number: NSC-15-1232R1

Title: Visual impairment in FOXG1-mutated patients and mice

Article Type: Research Paper

Section/Category: Disease-Oriented Neuroscience

Keywords: Rett syndrome, Autism, West syndrome, visual cortex, inhibitory interneurons, cortical blindness

Corresponding Author: Dr. Tommaso Pizzorusso, Ph.D.

Corresponding Author's Institution: University of Florence

First Author: Elena M Boggio

Order of Authors: Elena M Boggio; Laura Pancrazi; Caterina Lo Rizzo; Francesca Mari; Ilaria Meloni; Francesca Ariani; Anna Panighini; Elena Novelli; Enrica Strettoi; Joussef Hayek; Alessandra Rufa; Tommaso Pizzorusso, Ph.D.; Alessandra Renieri; Mario Costa

Abstract: The Forkead Box G1 (FOXG1) gene encodes for a DNA-binding transcription factor, essential for the development of the telencephalon in mammalian forebrain. Mutations in FOXG1 have been reported to be involved in the onset of Rett Syndrome, for which sequence alterations of MECP2 and CDKL5 are known. While visual alterations are not classical hallmarks of Rett syndrome, an increasing body of evidence shows visual impairment in patients and in MeCP2 and CDKL5 animal models. Herein we focused on the functional role of FOXG1 in the visual system of animal models (Foxg1+/Cre mice) and of a cohort of patients carrying FOXG1 mutations or deletions. Visual physiology of Foxg1+/Cre mice was assessed by visually evoked potentials, which revealed a significant reduction in response amplitude and visual acuity with respect to wild-type littermates. Morphological investigation showed abnormalities in the organization of excitatory/inhibitory circuits in the visual cortex. No alterations were observed in retinal structure. By examining a cohort of FOXG1-mutated patients by means of a panel of neuro-ophthalmological evaluations, we found that all of them exhibited visual alterations compatible with high level visual dysfunctions. In conclusion our data show that Foxg1 haploinsufficiency results in an impairment of mouse and patient visual function.

Response to Reviewers: Pisa February 27th 2016

Dear Editor,

We would like to thank the referees for the thoughtful critiques on our manuscript and for the opportunity to revise our work. Please find enclosed a revised version of our manuscript (NSC-15-1232) entitled “Visual impairment in FOXG1-mutated patients and mice” by Boggio et al. As requested, we performed additional experiments on retina and visual cortex in order to more quantitavely prove the structure specific

alterations and strengthen our conclusions. We included below a detailed response to the reviewer comments (in italics).
References have been updated and added as suggested by referees.

Sincerely, Tommaso Pizzorusso

Reviewer #1:

Major concerns

1. The description of the morphology of the five classes of retinal neurons would benefit from a quantitative approach amenable to statistical comparisons, similar to that performed for cortical GABAergic neurons in Fig. 4.

We performed the requested quantitative analysis that is now shown in fig. 4. The analysis was focussed on cells in the ganglion cell layer because this layer is known to be affected in Foxg1 null mice. No significant change in the overall number of cells, and in ganglion cells identified using the RBPMS cell type-specific antibody, was present in Foxg1 heterozygous mice

2. There are no explicit statements regarding blinding of investigators to mouse genotypes during data acquisition and analyses, the use of Power Analysis to determine sample sizes, and predetermined criteria to exclude data sets. These are all critical issues that need to be performed and explicitly reported as recommended (Landis et al. Nature 2012).

We included in the methods the following section:

Statistics and data collection.
Data were collected and analyzed by investigators blind to the genetic and treatment status of the animal. Only animals with significantly altered EEG or breath rate during VEP recordings were discarded. Sample size was estimated by power analysis using data present in the literature on VEP and inhibitory circuit alterations in mouse models of neurodevelopmental disorders. Animals were randomly assigned to the various experimental groups caring that littermates were divided in the different experimental groups. To analyze data we used the paired t-test (to compare two repeated measures on the same subjects) and the t-test (to compare between different subjects). ANOVA was used to compare many groups. P=0.05 was assumed as significance level. Statistical analysis was performed using the Sigma Stat (Systat, USA) software.

Minor concerns

1. Ambulatory people should be referred to as "individuals", not "patients" because they are not hospitalized.

We agree with the reviewer. The term patient was replaced by subject or individual along the entire paper.

2. "Normal" and "abnormal" have negative connotations. "Typical" and "atypical" are preferred.

We agree with the reviewer and the terms normal and abnormal were replaced by typical and atypical along the entire paper when refer to human subjects.

3. "Mental retardation" has negative connotations. "Intellectual disability" is preferred.

Again, we agree with the reviewer and "Mental retardation" was replaced by "Intellectual disability" along the entire paper.

4. More details are needed about the acquisition and analysis of brain MRI, EEG, and VEP data from individuals with FOXG1 mutations and typical controls (for comparisons).

We added a more complete description in the experimental procedures and in Table 1 legend. Morever we included the following paragraph in Results:

Visual performance in control subjects
All subjects with age older than 4 years showed a best corrected visual acuity between 20/20-20/25, color vision was 15/15 (Hishihara platelets), pupils were reactive, anterior segment and lenses were clear, fixation was stable and ocular motility was normal. Younger patients (age under 4 years) showed a good engagement for near and far visual stimuli, they were able to follow light and objects and were also able to reach or grasp objects of interest even if presented in a crowded surrounding.VEPs results in control subjects showed a mean latency of the P100 of 99.19 ms(range 90-105 ms); and a mean amplitude of the N75-P100 of 7,37 µV(range 5-10,1 µV).

5. More details are needed about the Foxg1-Cre heterozygous mice. For example, what does "Cre" means? Was the Foxg1 flanked by loxP sites ("floxed") and deleted by breeding with a Cre-expressing mouse line? In what cell type was Cre expressed? Also, more clarity is needed on the mouse breeding scheme: were male WT cross with female Foxg1-Cre, or viceversa?

We apologize for the lack of clarity and, as also requested by referee 2, these aspects are now described in the experimental procedure (animals) and in the results (section titled Reduced cortical VEP acuity in Foxg1 +/- Mice).
In synthesis; this mouse line was created by Herbert et al (now quoted in the manuscript) to facilitate genetic studies of telencephalic development by generating a mouse line, Foxg1–Cre, in which the sequence encoding the Cre recombinase is targeted to a locus expressed specifically in the telencephalon. The recombination pattern obtained with Foxg1–Cre mice matches the normal expression pattern of Foxg1, demonstrating the utility of this mouse for inducing tissue-specific recombination when crosses with loxP mouse lines.

6. The depth of the cortical electrode must be 100 microns, not nanometers.

We apologize; the text has now been corrected.

7. "O/N" should be spelled out.
Done

8. "Data not shown" should be presented.

A description of the cone morphology is now reported in the result section.

Reviewer #2: The results are interesting, however still preliminary. In brief the following points should be fully addressed before publication.

1) In the human data there is no mention of analysis of age matched typically developing subjects. These control data are essential and should be provided. Given the wide range of ages analyzed, the small group of patients and complete lack of control subjects, and the complete lack of quantitative unbiased analysis (like VEP), the conclusions are at best anecdotal and should be tone down.

Following the suggestions of the two referees we added a group of 20 age and sex matched control subjects who undergone a complete neuro-ophthalmological exam and flash VEPs. Data of control subjects were included in the material and methods section and results. Moreover value of latency and amplitude of flash VEPs have been added in table 1 including value of control subjects.

2) In figure 1, the authors show a significant reduction in the visual acuity in Foxg1+/Cre mice. They claimed that there is a strong reduction of the VEP response also at the low spatial frequency (0.03-0.05 c/deg) but they don't show any waveform or any statistical analysis regarding such data. The wave form in response to low spatial frequency should be presented for the two genotypes and analysis of maximal amplitude and the latency performed and discussed.

We agree with the referee. Waveforms are reported in fig. 1A and the stastistics of low-spatial frequency VEPs (0.1 c/deg) is reported in the results.

3) Figure 4 is not well explained and contains several incongruences. The authors highlighted a significant reduction of NeuN density in the supragranular layers, whereas in the figure legends they don't report such result. In the figure legends, the authors talked about bins, whereas in figure 4 they used cell distribution as x axis title. It is also unclear how they could fit the same number of bins between the two genotypes or what do they mean with cell distribution.

We agree that this analysis should be clarified. We have now recounted all our data based on cortical layers and added one mouse/group. Morever,

we included the statistical analysis of NeuN density (Fig. 4 legend) and of cortical thickness (in the text of the Results).

4) Based on the calbindin representative images (4D, left), this marker most likely stains also for pyramidal cells. How do the authors distinguish between the two cells population and make sure to quantify only the interneuron populations?

Considering the observation made by the reviewer and data present in the literature calling into question the specificity of calbindin as an interneuronal marker we preferred to remove calbindin analysis from the paper and substitute it with the general inhibitory marker GAD67.

5) Based on their NeuN cell density results, I would not had expected any major changed in sub-cell populations. Did the authors also quantify the overall number of interneurons with a GABA-GAD marker? What is it the cell density of the excitatory cells?

We quantified the overall density of inhibitory interneurons by GAD67 staining. No difference was present between genotype in any layer (Fig. 5D). It has to be noted that the changes that we observed with calretinin and parvalbumin go in opposite direction possibly explaining the lack of change in the overall population of GAD67 positive cells. Considering that Neu-N is reduced significantly in the upper layers, we infer that the reduction is mostly due to a reduction in excitatory cells.

6) In figure 5 the authors reported a reduction of spine density, however they should also report the overall cell morphology. Is the spine density reduced due to shrinkage of the pyramidal cells following the shortening of the cortical layer?

We checked cell diameter and no difference was present in cell body diameter (wt N= 25 cells 16.9 □m SEM 2.3, Foxg1+/Cre N=24 cells 15.8 □m SEM 2.6; t-test p=0.76).

7) Pag 12, line 60 :..consisting in a modestly thinner neocortex..". Looking at figure 4, FoxG1+/Cre mice are characterized by a major shrinkage of the neocortex. Did the authors quantify cortical thickness across multiple sections/animals?

Yes, there is a significantly thinner cortex (data in the Results section). This is prominently due to a reduction of layer II-III thickness associated with loss of Neu-N positive cells

8) In the introduction the authors should discuss more in depth the function of the foxg1 protein or the fact that different mutations of the FOXG1 gene -microdeletion and microduplication- can induce different phenotypes in humans. For example, microdeletions and point mutations of FOXG1 gene, that usually result in a shortage of the protein, disrupt normal brain development causing brain malformation and severe developmental problems. Microduplications of the same gene have been identified in infants with West syndrome and are characterized by severe epilepsy.

In the revised version of the manuscript we tried to better describe the FOXG1 congenital variant of Rett, as a member of the family of FOXG1 related disorder, also considering the space limitations imposed by the journal.

9) The experimental procedures are poorly written and lack essential information. Info about the mouse model should be added in the animal section and clearly stated that the foxg1 Cre+/- mouse line is a knock-in line resulting in decrease of expression of FOXG1 gene. The relative citation should be provided in the main text and methods section. The authors should state how many mice, retinas, sections, cells have been used in each experiment reported. Right now it is a bit confusing and not totally clear (for example where the three retinas from 3 mice or 2). Finally, in the immunohistochemistry section there is no information about acquisition parameters or quantification methods. How big are the bins for the interneurons analysis? How did the authors measure the spine density? per length of dendrite? How many spines, dendrites, cells did they count in each genotype?

We agree with the reviewer and the experimental procedures are now more detailed as requested.

10) Overall the introduction and discussion are poorly written and lack major citations. For example, the authors should discuss the papers showing that RTT models have a specific visual phenotype, like in Tropea et al. 2009, Durand et al., 2012; Krishnan et al., 2015 and the recently published LeBlanc et al. (Annals of Neurology 2015) reporting significant visual impairment in Rett Syndrome patients. Citations are also incomplete regarding disruption in interneuron circuits in Rett Syndrome. At a minimum, the authors should cite Durand et al., 2012, Tomassy et al., 2014 and Krishnan et al., 2015.

The quotations have been updated including the reference pointed out by the referee,

Minor points:
The whole text contains several for the mouse Foxg1 gene, human FOXG1 gene, and related proteins throughout the paper.

We clarified the nomenclature of Forkead BoxG1 (FOXG1in humans, Foxg1 in mice) gene in the abstract.

The last paragraph of the introduction is repetitive and doesn't describe clearly the goals and/or the results of the present paper.

We modified the paragraph according to the referee suggestion.

Scale bars needs to be added to figure 4 and figure 5.

Page 14, line 47-48: ".. PV immunoreactivity develops.. at P10..". Add a citation. It is usually believed that PV immunoreactivity in the visual cortex starts at eye opening, P12-P13.

We thank the reviewer for making us notice this mistake. The text has now been corrected:

PV immunoreactivity develops postnatally: in mice, it appears around eye opening at P13-P14 in intermediate layers, from which it expands to the upper and inner cortical layers at subsequent developmental stages.

Pisa February 27th 2016

Dear Editor,

We would like to thank the referees for the thoughtful critiques on our manuscript and for the opportunity to revise our work. Please find enclosed a revised version of our manuscript (NSC-15-1232) entitled “Visual impairment in FOXG1-mutated patients and mice” by Boggio et al.
As requested, we performed additional experiments on retina and visual cortex in order to more quantitavely prove the structure specific alterations and strengthen our conclusions. We included below a detailed response to the reviewer comments (in italics).
References have been updated and added as suggested by referees.

This manuscript is in accordance with the Authorship statement of ethical standards for manuscripts submitted to *Neuroscience.*

Sincerely, Tommaso Pizzorusso

Pisa February 27th 2016

Dear Editor,

We would like to thank the referees for the thoughtful critiques on our manuscript and for the opportunity to revise our work. Please find enclosed a revised version of our manuscript (NSC-15-1232) entitled "Visual impairment in FOXG1-mutated patients and mice" by Boggio et al.
As requested, we performed additional experiments on retina and visual cortex in order to more quantitavely prove the structure specific alterations and strengthen our conclusions. We included below a detailed response to the reviewer comments (in italics).
References have been updated and added as suggested by referees.

Sincerely, Tommaso Pizzorusso

Reviewer #1:

Major concerns

1. *The description of the morphology of the five classes of retinal neurons would benefit from a quantitative approach amenable to statistical comparisons, similar to that performed for cortical GABAergic neurons in Fig. 4.*

We performed the requested quantitative analysis that is now shown in fig. 4. The analysis was focussed on cells in the ganglion cell layer because this layer is known to be affected in *Foxg1* null mice. No significant change in the overall number of cells, and in ganglion cells identified using the RBPMS cell type-specific antibody, was present in *Foxg1* heterozygous mice

2. *There are no explicit statements regarding blinding of investigators to mouse genotypes during data acquisition and analyses, the use of Power Analysis to determine sample sizes, and predetermined criteria to exclude data sets. These are all critical issues that need to be performed and explicitly reported as recommended (Landis et al. Nature 2012).*

We included in the methods the following section:

Statistics and data collection.

Data were collected and analyzed by investigators blind to the genetic and treatment status of the animal. Only animals with significantly altered EEG or breath rate during VEP recordings were discarded. Sample size was estimated by power analysis using data present in the literature on VEP and inhibitory circuit alterations in mouse models of neurodevelopmental disorders. Animals were

randomly assigned to the various experimental groups caring that littermates were divided in the different experimental groups. To analyze data we used the paired t-test (to compare two repeated measures on the same subjects) and the t-test (to compare between different subjects). ANOVA was used to compare many groups. P=0.05 was assumed as significance level. Statistical analysis was performed using the Sigma Stat (Systat, USA) software.

Minor concerns

1. *Ambulatory people should be referred to as "individuals", not "patients" because they are not hospitalized.*

We agree with the reviewer. The term patient was replaced by subject or individual along the entire paper.

2. *"Normal" and "abnormal" have negative connotations. "Typical" and "atypical" are preferred.*

We agree with the reviewer and the terms normal and abnormal were replaced by typical and atypical along the entire paper when refer to human subjects.

3. *"Mental retardation" has negative connotations. "Intellectual disability" is preferred.*

Again, we agree with the reviewer and "Mental retardation" was replaced by "Intellectual disability" along the entire paper.

4. *More details are needed about the acquisition and analysis of brain MRI, EEG, and VEP data from individuals with FOXG1 mutations and typical controls (for comparisons).*

We added a more complete description in the experimental procedures and in Table 1 legend.
Morever we included the following paragraph in Results:

Visual performance in control subjects

All subjects with age older than 4 years showed a best corrected visual acuity between 20/20-20/25, color vision was 15/15 (Hishihara platelets), pupils were reactive, anterior segment and lenses were clear, fixation was stable and ocular motility was normal. Younger patients (age under 4 years) showed a good engagement for near and far visual stimuli, they were able to follow light and objects and were also able to reach or grasp objects of interest even if presented in a crowded surrounding.VEPs results in control subjects showed a mean latency of the P100 of 99.19 ms(range 90-105 ms); and a mean amplitude of the N75-P100 of 7,37 μV(range 5-10,1 μV).

5. *More details are needed about the Foxg1-Cre heterozygous mice. For example, what does "Cre" means? Was the Foxg1 flanked by loxP sites ("floxed") and deleted by breeding with a Cre-expressing mouse line? In what cell type was Cre expressed? Also, more clarity is needed on the mouse breeding scheme: were male WT cross with female Foxg1-Cre, or viceversa?*

We apologize for the lack of clarity and, as also requested by referee 2, these aspects are now described in the experimental procedure (animals) and in the results (section titled Reduced cortical VEP acuity in Foxg1 +/- Mice).

In synthesis; this mouse line was created by Herbert et al (now quoted in the manuscript) to facilitate genetic studies of telencephalic development by generating a mouse line, Foxg1–Cre, in which the sequence encoding the Cre recombinase is targeted to a locus expressed specifically in the telencephalon. The recombination pattern obtained with Foxg1–Cre mice matches the normal expression pattern of Foxg1, demonstrating the utility of this mouse for inducing tissue-specific recombination when crosses with loxP mouse lines.

6. *The depth of the cortical electrode must be 100 microns, not nanometers.*

We apologize; the text has now been corrected.

7. "O/N" *should* be spelled out.

Done

8. "Data not shown" should be presented.

A description of the cone morphology is now reported in the result section.

Reviewer #2: The results are interesting, however still preliminary. In brief the following points should be fully addressed before publication.

1) In the human data there is no mention of analysis of age matched typically developing subjects. These control data are essential and should be provided. Given the wide range of ages analyzed, the small group of patients and complete lack of control subjects, and the complete lack of quantitative unbiased analysis (like VEP), the conclusions are at best anecdotal and should be tone down.

Following the suggestions of the two referees we added a group of 20 age and sex matched control subjects who undergone a complete neuro-ophthalmological exam and flash VEPs. Data of control subjects were included in the material and methods section and results. Moreover

value of latency and amplitude of flash VEPs have been added in table 1 including value of control subjects.

2) In figure 1, the authors show a significant reduction in the visual acuity in Foxg1+/Cre mice. They claimed that there is a strong reduction of the VEP response also at the low spatial frequency (0.03-0.05 c/deg) but they don't show any waveform or any statistical analysis regarding such data. The wave form in response to low spatial frequency should be presented for the two genotypes and analysis of maximal amplitude and the latency performed and discussed.

We agree with the referee . Waveforms are reported in fig. 1A and the stastistics of low-spatial frequency VEPs (0.1 c/deg) is reported in the results.

3) Figure 4 is not well explained and contains several incongruences. The authors highlighted a significant reduction of NeuN density in the supragranular layers, whereas in the figure legends they don't report such result. In the figure legends, the authors talked about bins, whereas in figure 4 they used cell distribution as x axis title. It is also unclear how they could fit the same number of bins between the two genotypes or what do they mean with cell distribution.

We agree that this analysis should be clarified. We have now recounted all our data based on cortical layers and added one mouse/group. Morever, we included the statistical analysis of NeuN density (Fig. 4 legend) and of cortical thickness (in the text of the Results).

4) Based on the calbindin representative images (4D, left), this marker most likely stains also for pyramidal cells. How do the authors distinguish between the two cells population and make sure to quantify only the interneuron populations?

Considering the observation made by the reviewer and data present in the literature calling into question the specificity of calbindin as an interneuronal marker we preferred to remove calbindin analysis from the paper and substitute it with the general inhibitory marker GAD67.

5) Based on their NeuN cell density results, I would not had expected any major changed in sub-cell populations. Did the authors also quantify the overall number of interneurons with a GABA-GAD marker? What is it the cell density of the excitatory cells?

We quantified the overall density of inhibitory interneurons by GAD67 staining. No difference was present between genotype in any layer (Fig. 5D). It has to be noted that the changes that we observed with calretinin and parvalbumin go in opposite direction possibly explaining the lack of change in the overall population of GAD67 positive cells. Considering that Neu-N is reduced significantly in the upper layers, we infer that the reduction is mostly due to a reduction in excitatory cells.

6) In figure 5 the authors reported a reduction of spine density, however they should also report the overall cell morphology. Is the spine density reduced due to shrinkage of the pyramidal cells following the shortening of the cortical layer?

We checked cell diameter and no difference was present in cell body diameter (wt N= 25 cells 16.9 μm SEM 2.3, *Foxg1*$^{+/Cre}$ N=24 cells 15.8 μm SEM 2.6; t-test p=0.76).

7) Pag 12, line 60 :..consisting in a modestly thinner neocortex..". Looking at figure 4, FoxG1+/Cre mice are characterized by a major shrinkage of the neocortex. Did the authors quantify cortical thickness across multiple sections/animals?

Yes, there is a significantly thinner cortex (data in the Results section). This is prominently due to a reduction of layer II-III thickness associated with loss of Neu-N positive cells

8) In the introduction the authors should discuss more in depth the function of the foxg1 protein or the fact that different mutations of the FOXG1 gene -microdeletion and microduplication- can induce different phenotypes in humans. For example, microdeletions and point mutations of FOXG1 gene, that usually result in a shortage of the protein, disrupt normal brain development causing brain malformation and severe developmental problems. Microduplications of the same gene have been identified in infants with West syndrome and are characterized by severe epilepsy.

In the revised version of the manuscript we tried to better describe the FOXG1 congenital variant of Rett, as a member of the family of FOXG1 related disorder, also considering the space limitations imposed by the journal.

9) The experimental procedures are poorly written and lack essential information. Info about the mouse model should be added in the animal section and clearly stated that the foxg1 Cre+/- mouse line is a knock-in line resulting in decrease of expression of FOXG1 gene. The relative citation should be provided in the main text and methods section. The authors should state how many mice, retinas, sections, cells have been used in each experiment reported. Right now it is a bit confusing and not totally clear (for example where the three retinas from 3 mice or 2). Finally, in the immunohistochemistry section there is no information about acquisition parameters or quantification methods. How big are the bins for the interneurons analysis? How did the authors measure the spine density? per length of dendrite? How many spines, dendrites, cells did they count in each genotype?

We agree with the reviewer and the experimental procedures are now more detailed as requested.

10) Overall the introduction and discussion are poorly written and lack major citations. For example, the authors should discuss the papers showing that RTT models have a specific visual phenotype, like in Tropea et al. 2009, Durand et al., 2012; Krishnan et al., 2015 and the recently published LeBlanc et al. (Annals of Neurology 2015) reporting significant visual impairment in Rett Syndrome patients. Citations are also incomplete regarding disruption in interneuron circuits in Rett Syndrome. At a minimum, the authors should cite Durand et al., 2012, Tomassy et al., 2014 and Krishnan et al., 2015.

The quotations have been updated including the reference pointed out by the referee,

Minor points:
The whole text contains several for the mouse Foxg1 gene, human FOXG1 gene, and related proteins throughout the paper.

We clarified the nomenclature of Forkead Box G1 (FOXG1in humans, Foxg1 in mice) gene in the abstract.

The last paragraph of the introduction is repetitive and doesn't describe clearly the goals and/or the results of the present paper.

We modified the paragraph according to the referee suggestion.

Scale bars needs to be added to figure 4 and figure 5.

Page 14, line 47-48: ".. PV immunoreactivity develops.. at P10..". Add a citation. It is usually believed that PV immunoreactivity in the visual cortex starts at eye opening, P12-P13.

We thank the reviewer for making us notice this mistake. The text has now been corrected:
PV immunoreactivity develops postnatally: in mice, it appears around eye opening at P13-P14 in intermediate layers, from which it expands to the upper and inner cortical layers at subsequent developmental stages.

Highlights

1) *Foxg1* haploinsufficiency causes impairment of mouse and human visual function.
2) $Foxg1^{+/Cre}$ mice show defects in the visual cortex excitatory/inhibitory circuits.
3) *FOXG1*-related visual alterations are compatible with the blind-sight syndrome.

*Manuscript (Clear Copy)
Click here to view linked References

Visual impairment in *FOXG1*-mutated individuals and mice

Elena M Boggio[1,£,#], Laura Pancrazi [1,2#], Mariangela Gennaro [1,6], Caterina Lo Rizzo [3,4], Francesca Mari [3,4], Ilaria Meloni [3], Francesca Ariani [3,4], Anna Panighini[1], Elena Novelli [1],Martina Biagioni [1, 5], Enrica Strettoi [1], Joussef Hayek [7], Alessandra Rufa [5], Tommaso Pizzorusso [1,6*], Alessandra Renieri [3,4*] and Mario Costa [1,2]

1 CNR Neuroscience Institute, Pisa Italy

2 Scuola Normale Superiore, BioSNS lab, Pisa Italy

3 Medical Genetics, University of Siena, Siena, Italy

4 Genetica Medica, Azienda Ospedaliera Universitaria Senese, Siena, Italy

5 Tuscan Doctorate School, University of Firenze, Firenze, Italy

6 Eye Tracking and Visual Application Lab (EVAlab), University of Siena, Siena, Italy

7 NEUROFARBA Department, University of Firenze, Firenze, Italy

8 Child Neuropsychiatry Unit, University Hospital, AOUS, Siena, Italy

*Corresponding authors:

Tommaso Pizzorusso tommaso@in.cnr.it

Alessandra Renieri alessandra.renieri@unisi.it

# both authors equally contributed to the work

£ Current address: Dept of Veterinary Science, University of Turin

Abstract

The *Forkead Box G1* (*FOXG1*in humans, *Foxg1* in mice) gene encodes for a DNA−binding transcription factor, essential for the development of the telencephalon in mammalian forebrain. Mutations in *FOXG1* have been reported to be involved in the onset of Rett Syndrome, for which sequence alterations of *MECP2* and *CDKL5* are known. While visual alterations are not classical hallmarks of Rett syndrome, an increasing body of evidence shows visual impairment in patients and in *MeCP2*and *CDKL5* animal models. Herein we focused on the functional role of FOXG1 in the visual system of animal models (*Foxg1*$^{+/Cre}$ mice) and of a cohort of subjects carrying *FOXG1* mutations or deletions. Visual physiology of *Foxg1*$^{+/Cre}$ mice was assessed by visually evoked potentials, which revealed a significant reduction in response amplitude and visual acuity with respect to wild-type littermates. Morphological investigation showed abnormalities in the organization of excitatory/inhibitory circuits in the visual cortex. No alterations were observed in retinal structure. By examining a cohort of *FOXG1*-mutated individuals with a panel of neuro-ophthalmological assessments, we found that all of them exhibited visual alterations compatible with high level visual dysfunctions. In conclusion our data show that *Foxg1* haploinsufficiency results in an impairment of mouse and human visual cortical function.

Keywords: Rett syndrome, Autism, West syndrome, visual cortex, inhibitory interneurons, cortical blindness

Rett Syndrome (RTT) is a neurodevelopmental disorder representing one of the most common causes of intellectual disability in girls. Beside the classical form due to *MECP2* mutations, two other forms have been associated to specific molecular defects, namely the early-onset seizure variant, mostly due to *CDKL5* mutations, and the congenital variant, mostly due to *FOXG1* mutations. The association between the *FOXG1* gene (OMIM#164874) and the congenital variant of RTT is relatively recent (Ariani et al., 2008), and since its discovery an increasing number of patients with *FOXG1* point mutations have been reported. The human *FOXG1* gene is located in the 14q12 chromosome and encodes for a phylogenetically well conserved DNA-binding transcription factor of 489 aa. The mechanisms by which *FOXG1* mutations cause RTT are still unknown, however the presence of *FOXG1* on an autosomic chromosome suggests haploinsufficiency as a candidate for the aetio-pathological mechanisms of this RTT variant (Shoichet et al., 2005, De Filippis et al., 2012). Furthermore, a physical interaction between MeCP2 and FOXG1 has been demonstrated (Dastidar et al., 2012) suggesting that, at least in the Central Nervous system (CNS), an impairment in FOXG1-MeCP2 interaction could be critical for the development of RTT. Intriguingly, a recent report indicates that Foxg1 displays, together with a nuclear localization, a specific targeting to mitochondria. This finding sheds new light on the etiology of FOXG1-RTT and on the original mitochondrial dysfunction hypothesis for the RTT pathogenesis (Pancrazi et al., 2015).

Foxg1 presence is essential for the embryonic development of the telencephalon in mammalian forebrain (Xuan et al., 1995). Its expression is abundant since the early development, persisting at lower levels in the adult cortex including the visual areas (Shen et al., 2006). This pattern suggests that specific aspects of the RTT associated with *FOXG1* mutations might involve visual cortical circuits. Foxg1 is also necessary for the correct formation of the inner ear and the olfactory system (Pauley et al., 2006, Duggan et al., 2008) and the appropriate crossing of retinal ganglion cell axons during development (Pratt et al., 2004). Interestingly, recent data show that Foxg1 overexpression is associated with neurodevelopmental pathologies and autism (Mariani et al., 2015).

Foxg1 null mice were first obtained in 1995: while *Foxg1*$^{+/-}$ animals were believed to have a normal phenotype, *Foxg1*$^{-/-}$ mutants showed a dramatic reduction in the size of the cerebral hemispheres and died at birth. Due to the lethal phenotype, functional studies in null animals were initially restricted to the determination of the mechanisms influencing the forebrain size and the development of the telencephalon. More in depth analysis of the *Foxg1*$^{+/-}$ model showed microcephaly, hyperlocomotion, impaired habituation in the open field and a severe deficit in contextual fear conditioning, recapitulating some features of disorders derived from deregulation of

FOXG1 expression such as the congenital variant of RTT and West syndrome (Shen et al., 2006, Eagleson et al., 2007, Siegenthaler et al., 2008). These features suggested the possibility to use *Foxg1*$^{+/-}$ mutants as models for these diseases (Shen et al., 2006, Ariani et al., 2008, Bahi-Buisson et al., 2010, Mencarelli et al., 2010, Philippe et al., 2010, Le Guen et al., 2011a, Le Guen et al., 2011b, Striano et al., 2011, Tohyama et al., 2011).

Recent work showed that the visual system is altered in mouse models of RTT (Tropea et al., 2009, Durand et al., 2012, Krishnan et al., 2015) providing the opportunity to use the visual system to investigate the patho-physiology of RTT and to improve objective patient evaluation. Indeed, a specific cortical processing deficit has been discovered using pattern reversal VEPs in RTT patients. Importantly, amplitude and latency of VEP waveforms are related to disease stage, clinical severity and MECP2 mutation (LeBlanc et al., 2015). The hypothesis that *FOXG1* mutations affects visual development is also supported by data showing that in West syndrome patients, altered VEPs and poor visual behavior are hallmarks of the pathology (de Freitas Dotto et al., 2014). These data prompted us to analyze whether visual deficits were also present in Foxg1 RTT patients and in *Foxg1*$^{+/-}$mice. *FOXG1* subject's visual behavior suggested a high level visual dysfunction compatible with the blind-sight syndrome occurring in individuals with extensive damage of primary visual cortex and consisting in loss of awareness for visual stimuli. Similarly, mouse studies point to a severe alteration in the development of cortical inhibitory and excitatory circuits.The results of this study show that cortical visual impairments occur in both patients and animal model of RTT.

Experimental procedures

Subjects

FOXG1 subjects: Eight subjects (5 females and 3 males) with a *FOXG1* mutation were enrolled in the study. Age ranged from 9 months to 22 years (Table 1). All subjects had a clinical diagnosis of the congenital variant of RTT, with severe intellectual disability with early regression phase, severe microcephaly (range -3SD/-8SD) mostly postnatal, stereotypic handand tongue movements. One subject showed generalized epileptic seizures. Sleep disturbances were present in 5 out of 6 individuals in whom the information was collected. Brain MRI was available for 6 cases. It was typical in one while the other 5 showed corpus callosum agenesis or hypoplasia and other brain asymmetries (Table 1). Menstrual disorders are not reported in the only girlin post-pubertal age (patient 8).

Four subjects showed a 14q12 micro deletion involving the FOXG1 gene ranging in size from 1.1Mb to 6.73Mb; four showed a point mutation predicted to lead to a truncation of the protein (Table 1).

Controls were 20 subjects (10 males and 10 females, mean age 7.8 years; range12 months-22 years). None of them reported neurological problems, seizures, visual system diseases or history of pre- or perinatal illness. Subjects with refractive errors exceeding ± 1.5 diopters and strabismus were excluded. Regular neuro-ophthalmologic assessments were performed in each subject, including tests of visual acuity, color sensitivity, pupil reactivity, ocular alignment, fixation and motility, slit lamp evaluation, confrontation visual field testing, fundoscopy and recording of standard flash VEPs (Celesia, 1982, Lenassi et al., 2008).

1) Patient clinical assessment: Genetic counseling and clinical assessment were performed for 5 out of 8 subjects by the same clinical geneticists (AR and MF) and child neuropsychiatrist (JH). Clinical data of the remaining 3 patients were collected through clinical reports provided bythe families (patients 1,2,5).

2) Visual Assessment: Clinical neuro-ophthalmologic data of each subject, evaluated by an experienced neuro-ophthalmologist (AR),were collected, together with an extensive parents' interview, specificfor visual abilities impairment. Patients were approached gradually by planning several sections of examination or observation. The following visual tests were performed: refractive errors measurement (by cycloplegia and correction with appropriate lenses); an estimate of visual acuity and color vision (obtained using a modified form of forced choice-preferential

looking method); ocular alignment and fixation; oculo-cephalic reflexes; optokinetic nystagmus (when possible), cranial nerve examination; pupil reactivity evaluation; slit lamp examination; dilated fundoscopy. An estimation of visual field extension and subject's interest towards colored or familial stimuli compared to unfamiliar or non-colored stimuli was obtained during the examination; finally, visual engagement and visual-manual coordination were also evaluated. Brain MRI, EEG and flash VEP datawere collected whenever the examination was possible.

Animals

The Foxg1-cre line was created by replacing the intron-less Foxg1 coding region (expressed specifically in the telencephalic cells) with cre recombinase, resulting in a *Foxg1* heterozygous mouse with reduced expression of Foxg1 (Hebert and McConnell, 2000).
Foxg1$^{+/Cre}$ mice founders were a generous gift from Dr. Vania Broccoli. Animals were housed in a 12-h light/dark cycle with free access to food and water. All the experiments were carried out in accordance with the directives the European Community Council (86/609/EEC) and approved by the Italian Ministry of Health. All mice used in this study were generated by heterozygous wild type matings of the original *Foxg1*^{Cre}background (C57BL/6J)male with a wild type C57BL/6J female. This breeding scheme was used since the heterozygous animals show behavioral abnormalities in the parental care. C57BL/6J (wild type) mice were purchased from the Jackson Laboratories (Bar Harbor, ME, USA).

Statistics and data collection.

Data were collected and analyzed by investigators blind to the genetic and treatment status of the animal. Only animals with significantly altered EEG or breath rate during VEP recordings were discarded. Sample size was estimated by power analysis using data present in the literature on VEP and inhibitory circuit alterations in mouse models of neurodevelopmental disorders. Animals were randomly assigned to the various experimental groups caring that littermates were divided in the different experimental groups. To analyze data we used the paired t-test (to compare two repeated measures on the same subjects) and the t-test (to compare between different subjects). ANOVA was used to compare many groups. P=0.05 was assumed as significance level. Statistical analysis was performed using the Sigma Stat (Systat, USA) software.

Visually evoked potentials

Mice were anesthetized with an intraperitoneal injection of 20% urethane and mounted in a stereotaxic apparatus allowing a full view of the visual stimulus. After carefully removing a portion of the skull overlying the binocular visual cortex while leaving the dura mater intact, a glass-pulled recording electrode filled with NaCl (3 M) was inserted into the visual cortex perpendicularly to the stereotaxic plane. The electrode was inserted 100 μm deep from pial surface and 2.7-3 mm lateral in correspondence to lambda. The electrical signals were amplified (10,000-fold), band-pass filtered (0.3–100 Hz), digitized, and averaged (at least 75 events in blocks of 5 each). The transient VEPs in response to an abrupt contrast reversal (1 Hz) were evaluated by measuring the peak-to-trough amplitude. The visual stimuli consisted of horizontal gratings of different spatial frequencies and contrasts generated by a visual stimulator interface (VSG2:2 card; Cambridge Research System, Cheshire, UK) and presented on a monitor (Sony model CPD-G520) placed 20 cm in front of the animal.

Immunohistochemistry on visual cortex of *Foxg1*$^{+/+}$ and *Foxg1*$^{+/Cre}$ mice

Animals were deeply anaesthetized and perfused transcardially with PBS 1X followed by 4% paraformaldehyde. Brains were removed, post-fixed in the same fixative at 4°C and cryoprotected by immersion in 30% sucrose. Forty μm coronal sections were cut on a freezing microtome and processed for immunohistochemistry. Free floating sections were incubated for 1-2 hours in a blocking solution (10% BSA, 0,3% Triton X-100 in PBS), then in the primary antibody solution O/N. The following day, the sections were incubated with appropriate secondary antibodies, mounted on glass slides and acquired with a Leica TCS-SP confocal microscope. The images were analyzed with ImageJ software. The following primary Abs were used: NeuN (1:500; Millipore, Billerica, MA, USA), MeCP2 (1:1000 cat. n. M 9317 Sigma Aldrich, Germany), parvalbumin (1:1000, Sigma Aldrich, Germany), calretinin (1:1000, Swant, Switzerland) and GAD67 (1:500, Chemicon, USA). Secondary antibodies used were Alexa Fluor 488 and Alexa Fluor 555 from Invitrogen.

Immunohistochemistry on retinal sections of *Foxg1*$^{+/+}$ and *Foxg1*$^{+/Cre}$ mice

Whole eyes were removed from deeply anesthetized mice (4 *Foxg1*$^{+/Cre}$ and 4 wt mice), cut at the ora serrata and fixed for 1 hr in 4% paraformaldehyde. The anterior segments were removed, the eye cups rinsed in 0.1M phosphate buffer (PB), cryoprotected in 30% sucrose, infiltrated in OCT and snap frozen in isopentane/dry ice. Afterwards, the eye cups were sectioned vertically at 12 μm on a Leica cryostat. The sections were collected on coated slides, processed for immunofluorescence using a panel of primary antibodies and reacted with appropriated secondary

antibodies conjugated with Alexa Fluor 488 (from Invitrogen), Rodamine RedX or Cy3 (from Jackson). Selected sections were counterstained with micromolar solutions of Ethidium homodimer-1 or BOBO 1-iodide nuclear dyes (from Invitrogen). All preparations were screened with a Zeiss Axioplan microscope equipped with a colorAxioplan camera. Selected sections were imaged at high resolution by confocal microscopy or with a Zeiss Apotome apparatus. The following antibodies were used: for photoreceptors: rhodopsin (RET-P1Sigma #O4886) and cone-specific L and M opsins (Millipore #AB5404 and #AB5407); for rod bipolar cells: PKCα (Sigma #P4334);for selected cone bipolar cell types: synaptotagmin2 - ZNP1 (ZIRC, Zebrafish International Resource Center); for amacrine cells:calretinin (Swant #7699/4); for cholinergic amacrine cells:ChAT (Chemicon #AB114P); for horizontal and ganglion cells:Neurofilament 200 (Sigma #N0142); for ganglion cells: SMI-32 (Covance#SMI32R) and Brn3 (Santa Cruz sc-6026); for synaptic ribbons: CtBP2 (Ribeye, BD Transduction Lab. #612044);for mitochondria: SOD2 (Invitrogen#A21990).

Counts of cells in the ganglion cell layer (GCL)

Additional *Foxg1*$^{+/+}$ and *Foxg1*$^{+/Cre}$ mice were used for counting cells in the ganglion cell layer (GCL) following published protocols (Damiani et al., 2012, Rodriguez et al., 2014). Briefly, paraformaldheyde fixed retinas (n=3 per strain, each from a different animal) were isolated from eye cups, the vitreous removed and 4 partial cuts made to delimitate the dorsal, nasal, ventral and temporal quadrants. After washes in 0.01M PBS, the retinas were blocked overnight at 4°C in a solution containing 0.5% Triton X-100 and 5% goat serum. Then, they were incubated for 6 days at 4°C with an anti-RNA binding protein (RBPMS), guinea pig antibody (Phospho Solutions, CO, USA), specific for GCs (diluted 1:500), with 1% serum and 0.1% Triton X-100. After 3x20' washing in PBS, the retinas were incubated in Alexa Fluor 488-conjugated goat anti-guinea pig secondary antibody (Vector Laboratories, Burlingame, CA) diluted 1:800, washed 3x20' in PBS and counterstained for 2 hrs with Ethidium homodimer 1 (Vector Laboratories), diluted 1:1,000. After washing, retinal samples were finally mounted "ganglion cells up" in Vectashield. Retinal profiles of whole mount preparations were imaged in bright field with an Axiocam camera attached to a Zeiss microscope, using a 1.25x objective. Retinal areas were then measured on image tiff files using the edge detector tool of a Metamorph® routine. Flat-mounted retinas were imaged with a Zeiss Apotome fluorescence microscope using a 40x/1.5 n.a. Plan Neofluar oil objective. Five focal series of images (each covering a retinal area of 224 x 168 µm) were acquired in each of the four retinal quadrants at regular intervals from the periphery towards the optic nerve head. Serial optical sections (10-20), 0.5 µm apart, covering the thickness of the GCL were obtained. Projection images

were than generated and used for counting separately RBPMS positive cells (labelled green) and the nuclei of all the neurons in the layer, (labelled red), and comprising also those of displaced amacrine cells. The nuclei of blood vessel cells were excluded based on their typical elongated shape, small size and high brightness. Serial optical sections were used to count cells by navigating through z-stacks of the GCL in central retina areas characterized by elevated cell density.Total numbers of cells per retina were obtained multiplying average cellular densities by corresponding retinal areas.

Dendritic spine analysis.

Animals (n=3 for each genotype) were deeply anesthetized and perfused through the heart with 4% paraformaldehyde. A block of visual cortex was sectioned in the coronal plane into 300-μm-thick slices by using a vibratome. The lipophilic dye 1,1′-dioctadecyl-3,3,3′,3-tetramethylindocarbocyanine (DiI) (Invitrogen) was coated onto tungsten particles (diameter 1.1 μm; Bio-Rad) according to Gan et al. (Gan et al., 2000). DiI-coated particles were delivered to the slices by using a Helios Gene Gun System (Bio-Rad). A polycarbonate filter with a 3.0-μm pore size (Molecular Probes) was inserted between the gun and the preparation on a platform to remove clusters of large particles. Density of labeling was controlled by gas pressure (80 psi of helium). After labeling, slices were fixed in 4% paraformaldehyde. Labeled structures were analyzed by confocal microscopy. Images of basal dendrites of layer 2/3 pyramidal cells were acquired, stacked (0.5 μm step), and then analyzed with ImageJ. A total of 49 cells were counted; at least 6 dendrites per neuron were analyzed for a total number of 8820 spines. We measured the average spine lengths and densities (number of spines per length of dendrite) for each animal and calculated the mean per group.

Results

Visual performance in control subjects

All subjects with age older than 4 years showed a best corrected visual acuity between 20/20-20/25, color vision was 15/15 (Hishihara platelets), pupils were reactive, anterior segment and lenses were clear, fixation was stable and ocular motility was normal. Younger patients (age under 4 years) showed a good engagement for near and far visual stimuli, they were able to follow light and objects and were also able to reach or grasp objects of interest even if presented in a crowded surrounding. VEPs results in control subjects showed a mean latency of the P100 of 99.19 ms(range 90-105 ms); and a mean amplitude of the N75-P100 of 7,37 µV(range 5-10,1 µV).

Visual impairment in patients with *FOXG1* mutations

Considering that West syndrome patients carrying unbalanced levels of FOXG1 show visual impairment and that RTT models show abnormal development and plasticity of the visual system (LeBlanc et al., 2015), we decided to investigate whether patients with FOXG1 mutations displayed visual atypicalities (Castano et al., 2000). In all patients (Table 1), visual attention and engagement worsened with fatigue both when observed during examination and as reported by parents. Patients were apparently receptive to near (within reaching) visual stimuli that captured their attention. Actually, bright colored stimuli and moving objects (particularly when presented at short distance) were preferred. Patients' attention and awareness strongly decreased for far visual stimuli particularly when they were assembled with other objects (crowded surrounding). In these conditions, acoustic stimuli favored a brief visual engagement. Four patients out of eight demonstrated an inconstant ability to recognize familial faces (essentially parents), as observed during examination and reported by parents (Table 1). All patients had a variable dissociation between looking and reaching and demonstrated reduced or absent visual contact. All patients except one (#7) showed scarce visual engagement and no voluntary gazing toward surrounding visual stimuli. However, they were able to avoid obstacles or had a reaction of defense. They also showed an asymmetrical refractive defect between the two eyes. Four out of eight patients were photophobic and one showed compulsive gazing to bright light (#5). Anterior segment was typical in all patients. Pupils were reactive in seven out of eight cases. A jerk nystagmus was present in one patient (#2). Variable degrees of eyes misalignment and strabismus (exo and esotropia) were previously diagnosed in all patients. One patient presented a congenital oculomandibular syncinesia (#3). At fundoscopy, three patients showed smaller shape but typical appearing optic discs. Flash

VEPs, performed in three out of eight patients, were in the range of controls (see table 1). EEG showed epileptic changes particularly in occipital parietal and temporal parietal regions in two patients. These data prompted us to further characterize visual impairment and uncover the underlying neural defects exploiting a mouse model of *Foxg1* haploinsufficiency.

Reduced cortical VEP acuity in *Foxg1*$^{+/-}$ Mice.

To investigate possible consequences of the Foxg1 haploinsufficiency on visual function, we analyzed visual responses by recording Visually Evoked Potentials (VEP), a well-established technique for measuring overall visual function in mammals (Porciatti et al., 1999). Three Foxg1 heterozygous models (*Foxg1*$^{+/tet}$, *Foxg1*$^{+/lacZ}$ and *Foxg1*$^{+/cre}$) showing similar phenotype have been described in the literature (Shen et al., 2006, Eagleson et al., 2007). Among them, we choose the widely used *Foxg1*$^{+/Cre}$ mice on a C57/BL6J background, which shows the most evident anatomical alterations of the cerebral cortex (Eagleson et al., 2007). Heterozygous mice were chosen because they better recapitulate the patient condition, insofar homozygous animals show birth lethality and a dramatic reduction in the size of the cerebral hemispheres.

As expected, VEP responses to alternating gratings decreased in amplitude in response to increments of the spatial frequency of the stimulus (Fig. 1). As shown in Fig. 1A, VEP transient amplitude is plotted against the spatial frequency log and visual acuity is taken as the spatial frequency that coincides with the extrapolation to zero amplitude of the linear regression. Visual acuity was significantly reduced in P30 *Foxg1*$^{+/Cre}$ mice compared to wild-type littermates (*Foxg1*$^{+/Cre}$, 0.20 +/- 0.05 cycles/degree, n=9; WT, 0.51 cycles/degree, n=5; *, P=0.01, t-test, Fig. 1B). Moreover, VEP amplitudes at low spatial frequency were strongly diminished in *Foxg1*$^{+/Cre}$ mice (0.1 c/deg, wt 166.3 μV SEM 18.1, *Foxg1*$^{+/Cre}$ 18.1 μV SEM4.6; t-test, $p<0.001$). These data suggest that FOXG1 mutations could result in visual impairments in mice as in humans.

Retinal morphology in *Foxg1*$^{+/Cre}$ and wt mice.

To assess whether *Foxg1* haploinsufficiency results into evident abnormalities in retinal morphological organization, we probed retinal sections of *Foxg1*$^{+/Cre}$ mice and wild type littermates (n=3 per mice, per strain) with a panel of antibodies, comprising well established cell-type specific markers, indicators of retinal lamination and constituents of retinal synaptic contacts (Jeon et al., 1998, tom Dieck and Brandstatter, 2006, Wassle et al., 2009, Barone et al., 2012).

Retinal neurons of all the five classes (photoreceptors, horizontal, bipolar, amacrine and ganglion cells), were labeled and compared among the two strains (Fig. 2, 3). None of the used retinal markers revealed obvious differences in the thickness of retinal layers, in their lamination pattern or in the morphology of individual cell types, between mutant and wt mice. Rhodopsin antibodies and ethidium nuclear staining highlighted a regular array of rod photoreceptors with no signs of degeneration (Fig.2, A-B). Cones displayed the normal, elongated morphology with outer segments of adequate length and orientation. Similarly, the main neurons of the retino-fugal ("vertical") pathway, and namely rod bipolars (Fig. 3, A-B) and types of cone bipolars belonging to the "On" and "Off" functional varieties (C, D), had well ramified dendrites; their axonal arbors terminated in the appropriate sublaminae of the inner plexiform layer. Cholinergic processes, constituted by the dendrites of starburst amacrine cells, retained the characteristic distribution in two parallel bands precisely located at 1/3 and 2/3 of the inner plexiform layer (Fig.3, E and F). Calretinin staining revealed a third tier of processes, regularly positioned between the two cholinergic bands (Fig. 3, C and D). Ribeye, a marker of ribbons at retinal glutamatergic synapses (established by photoreceptors and bipolar cells) had the expected distribution in the outer and inner retina (Figure 3, A and B). Particular attention was paid to the analysis of the morphology and the number of ganglion cells (GCs), known to display abnormalities in axonal projections in homozygous mice (Pratt et al., 2004, Tian et al., 2008). SMI-32 anti-neurofilament antibodies highlighted a tier of large-size cell bodies corresponding to alpha-like ganglion cells, while immunolabeling for Brn3B, the transcription factor selectively expressed in these neurons (Xiang et al., 1993) showed a similar pattern of nuclear staining in the ganglion cell layer (GCL) of mutant and control retinas (Fig.2 C-D). Similarly, immunostaining with 200 kDa neurofilament antibodies showed a regular arrangement of cell bodies in theGCL, the expected bundles of axons in the optic fiber layer and profuse dendritic ramifications in the inner plexiform layer (Fig.3, E-F).The morphology of the optic nerve head in mutant mice appeared normal as well (Fig.2 A).

The GCL contains amacrine and ganglion cells, approximately in equal number in the rodent retina. Cell counts of retinal whole mounts (Fig. 4) from *Foxg1*$^{+/Cre}$ (n=3 retinas) and *Foxg1*$^{+/+}$ (wt) mice (n=3) demonstrated that the two strains did not differ in the absolute number of cells in the GCL (*Foxg1*$^{+/Cre}$ 106300, SEM 5369; *Foxg1*$^{+/+}$115475 cells SEM 4803, t-test; p=0.27; Fig.4 A-C). Selective counts of GCs, labeled with a RBPMS cell type-specific antibody, showed overlapping numbers of these neurons in mutant and wt strains (Fig.4 D). Noticeably, the numbers obtained here are not different from previously published data accounting for the total number of cells in the GCL (Jeon et al., 1998) and of GCs (Williams et al., 1998) of C57Bl6 mice.

In conclusion, no changes in general organization, architecture and pattern of lamination were observed in retinas of *Foxg1*$^{+/Cre}$ mice, which appeared undistinguishable from those of their wt littermates. The heterozygous expression of FoxG1 does not affect the total number of cells in the innermost retinal layer.

Morphological analysis of the visual cortex of *Foxg1*$^{+/Cre}$ mice.

Prompted by the strong functional impairment in cortical VEPs, we investigated the architecture of excitatory and inhibitory neurons in the visual cortex of *Foxg1* haploinsufficient mice.

As a general neuronal marker, we assessed the pattern of Neu-N immunostaining in P30 *Foxg1*$^{+/Cre}$ mice. As already reported (Eagleson et al., 2007), the visual cortex is thinner in this line of mutants.(wt 914.3 μm SEM 12.6; *Foxg1*$^{+/Cre}$ 747.9 μm SEM 29.8; n=4 for each group, t-test p=0.002). To determine the occurrence of layer-specific effects of *Foxg*1 haploinsufficiency on neuronal density, we quantified Neu-N positive neurons along the cortical depth. As shown in Fig. 5A, a significant reduction specific for layer II-III and layer IV was found in the mutant mice as compared to wt littermates.

To assess whether morphological defects were associated with specific neuronal populations, we first studied markers of inhibitory interneurons since disruption in interneuron circuits has been found in RTT mouse models (Durand et al., 2012, Tomassy et al., 2014, Krishnan et al., 2015), and then we investigated alterations in dendritic spines of excitatory pyramidal cells.

Calretinin (CR), parvalbumin (PV) and GAD67 immunostaining. Since maturation of cortical inhibition in visual areas is correlated with maturation of visual acuity and defects in cortical inhibition have been found in other mouse models of RTT (Dani et al., 2005, Lonetti et al., 2010), we decided to investigate the number of cortical inhibitory cells in *Foxg1*$^{+/Cre}$ mice. Therefore, we estimated the density of CR, PVand GAD67 positive cells in the visual cortex at P30. CR immunostaining highlighted a significant increase in the interneuron density in the layers II-III and VI of the *Foxg1*$^{+/Cre}$ cortex with respect to wt (Fig. 5B). By contrast, we observed a reduction of PV positive cell density in layers II-III of the visual cortex (Fig. 5C). The total number of inhibitory cells calculated using GAD67 immunohistochemistry was not affected in heterozygous *Foxg1*$^{+/Cre}$ mice (Fig. 5D).

Dendritic spine density and length. Alterations in density and size of dendritic spines have been found in *Mecp2* mouse models of Rett Syndrome (Belichenko et al., 2009, Landi et al., 2011) and

also in many other models of neurodevelopmental disorders (Fiala et al., 2002). To investigate morphological alterations induced by Foxg1 haploinsufficiency, we evaluated by diolistic labeling the spine density and length in the basal dendrites of pyramidal cells (layer 2/3) in visual cortices of *Foxg1*$^{+/Cre}$ mice and wt littermates. As indicated in Fig. 6, no differences was present in spine length between the two genotypes (Fig. 6C) but a significant decrease in spine density was measured in *Foxg1*$^{+/Cre}$ as compared to wt mice (Fig. 6B). No difference was present in cell body diameter (wt N= 25 cells 16.9 μm SEM 2.3, *Foxg1*$^{+/Cre}$ N=24 cells 15.8 μm SEM 2.6; t-test p=0.76).

These results indicate that the severe impairment of visual acuity caused by Foxg1 haploinsufficiency is likely to be due to defects in the morphological organization of visual cortical neurons.

Discussion

In this report we demonstrate for the first time the functional consequences of *Foxg1* haploinsufficiency in the visual system of *Foxg1*$^{+/Cre}$ mice and a visual impairment in a cohort of Rett individuals presenting genetic alteration on *FOXG1*. Previous reports showed minor alterations in haploinsufficent animals consisting in a modestly thinner neocortex and reduced dentate gyrus size. To address this issue, we measured the visual acuity of *Foxg1*$^{+/Cre}$ mice and their wild type littermates by means of Visually Evoked Potentials (VEPs). Our results show that *Foxg1*$^{+/Cre}$ mice have a severe impairment in visual acuity and that the origin of such an impairment in visual function is not likely to reside in the retina, as retinal organization in these animals is normal. Indeed, retinal structure is qualitatively and quantitatively normal in *Foxg1*$^{+/Cre}$ mice, and previous work showed that loss of a single *Foxg1*allele does not impair development of retinofugal axons (Tian et al., 2008). Consistently with the animal model, all the examined patients with *FOXG1* haploinsufficiency also show a visual impairment, with some common peculiarities. Such impairment seems to be principally caused by abnormal elaboration of visual signals in cortical areas.

Visual alterations in *FOXG1* mutated subjects

A common visual behavior reported in these subjects by relatives is the apparent lack of interest for any visual stimulus, often interpreted as low vision or narrowed visual field. This visual behavior

was better characterized in our subjects who mainly showed a scarce eye engagement, inconstant recognition of familial faces, and a general limited awareness to visual stimuli anywhere in the visual field, particularly when far and crowded. Despite a limited visual capacity, they were able to avoid obstacles and catch objects whenever positioned in neighboring space. The loss of attention and awareness for visual stimuli associated with the inability to disambiguate crowded objects or complex shapes; the inability of immediate recognition of familial faces, but the preserved interest and correct reaching or grasping toward colored stimuli and moving objects might suggest a condition resembling "blindsight". Blindsight syndrome is a well-recognized neuro-ophthalmological defect, which occurs upon extensive damage of the primary visual cortex (V1). Blindsight refers to the ability of cortically blind patients (bearing a primary visual cortex damage) to use extra striate visual information in guiding behaviors but in the absence of conscious object identification (Weiskrantz, 2009). Human blind-sight subjects are able to orient to and even answer questions about stimuli presented to the blind visual field. However, they are entirely unaware of the stimuli to which they are responding. Another characteristic of blindsight is that subjects can discriminate simple objects on the basis of their spatial frequency, shape, texture and color(Dineen and Keating, 1981), but they have lost the ability to identify more elaborate visual attributes, such as the capacity to visually recognize complex shapes or crowded objects, foods and familial faces. Moreover, blindsight patients well maintain reflexive saccades and motion perception, suggestingthat a residual network elaborating some visual information remains active even in case of extensive striate cortex lesions. The latter supports visually guided behaviors in the absence of awareness for visual stimuli. At least two separate pathways, and namely the retino-collicular and retino-geniculate pathways, reach the extrastriate cortex independently from the primary visual cortex, projecting to themotion area V5/MT in the medial temporal lobe. These connectionsmay represent theunconscious part of the dorsal 'where' visual stream, whereas the consciouscounterpart passes through the primary visual cortex before reachingthe V5/MT area. The extrastriate blind-sight pathways could be active in the *FOXG1* patients studied here, who indeed are attracted by colored and moving targets. On the contrary, their scarce awareness to visual stimuli might indicate a functional impairment of the striate visual pathway in the absence of retino-geniculate dysfunctions. This hypothesis (although not sustained by the demonstration of a structural damage of the occipital lobe detected by MRI) would suggest a functional impairment or incomplete maturation of the striate cortex as reinforced by the present results in the murine model.

Another visual system change in the human subjects studied here is the occurrence of ocular malformations, such as strabismus, oculo-mandibular syncinesias and small optic discs. These anomalies (observed in three individuals*)*, together with other cerebral malformations (i.e. corpus

callosum hypoplasia) may represent the expression of a global immaturity of the brain due to *FOXG1* mutations.

Cortical architecture is defective in *Foxg1*$^{+/Cre}$ mice

Retinal structure appeared normal in *Foxg1*$^{+/Cre}$ mice, with no apparent anomalies in cell type distribution, laminar organization and numerical deficit in GCs that could explain the visual abnormalities On the contrary, morphological studies showed significant changes in NeuN, PV and CR positive cells distribution in the visual cortex of *Foxg1*$^{+/Cre}$ mice compared to wild type animals. PV and CR are calcium binding proteins that serve as calcium buffers and label main subpopulations of GABA-ergic cortical interneurons. PV immunoreactivity develops postnatally: in mice, it appears around eye opening at P13-P14 in intermediate layers, from which it expands to the upper and inner cortical layers at subsequent developmental stages. In the visual cortex, PV positive cell maturation occurs during the critical period of ocular dominance plasticity and manipulations that accelerate or delay the time course of the critical period correspondingly regulate developmental maturation of PV cells. The decrease in PV cell density in uppermost layers and the increase in CR positive cells of *Foxg1*$^{+/Cre}$cortex suggest that Foxg1 haploinsufficiency results in an impairment in inhibitory circuitry maturation. PV+ synapses are usually perisomatic and PV+ pattern of innervation of pyramidal cells is engaged in controlof the spiking pattern. Their reciprocal and extensive connections can regulate the timing of activity in the cortex. Hence, we can speculate that the epileptic phenotype observed in *FOXG1* mutated patients (Brunetti-Pierri et al., 2011, Guerrini and Parrini, 2012) may be linked to a defective PV positive cells maturation. Conversely, CR positive cells usually synapse on dendrites; thus, the observed increase in CR positive cells in the lower layers of the *Foxg1*$^{+/Cre}$ cortex may cause a local alteration in cortical inhibition. Intriguingly, analysis of GAD67 positive neurons showed that the total number of inhibitory cells is preserved in *Foxg1*$^{+/Cre}$ mice. Thus, the reduction of NeuN positive neurons in the superficial layers is likely due to alterations of excitatory cells.

To further analyze the excitatory phenotype in *Foxg1*$^{+/Cre}$ primary visual cortex, we evaluated dendritic spine density and length in layer 2/3 pyramidal neurons. In the cerebral cortex, more than 90% of excitatory synapses terminate on spines. Spine density in the mouse neocortex increases during the second and third week of life and is followed by a period of major spine pruning and loss. In the primary visual cortex, dendritic spine density and morphology are developmentally regulated: they are plastic during young ages and become remarkably stable in adulthood. Our

results demonstrate a decrease in spine density in *Foxg1*$^{+/Cre}$ primary visual cortex compared to wild type animals.

Altogether, these results suggest that *Foxg1* haploinsufficiency causes alterations in both inhibitory and excitatory cells. Interestingly, alterations in inhibitory and excitatory synapses have been described in other mouse models of RTT as well as in a human disease model (iPSCs) obtained by genetic reprogramming of *FOXG1*-mutated patient fibroblasts (Patriarchi et al., 2015). In *MeCP2-KO* animals, the cortical excitatory input is reduced whilst the total inhibitory input is enhanced, leading to a shift of the homeostatic balance between excitation and inhibition in favor of inhibition. Moreover, MeCP2-deficient cortical and hippocampal neurons have fewer dendritic spines. *CDKL5*, the other gene found mutated in some cases of RTT, codes for a protein that has been demonstrated to localize at excitatory synapses, where it contributes to correct dendritic spine structure and synapse activity. *CDKL5* knockdown in cultured hippocampal neurons results in aberrant spine morphology (Chen et al., 2010) and unstable dendritic spines (Della Sala et al., 2015). Intriguingly, the analysis of novel mouse models carrying *Cdkl5* deletion showed alterations in sensory evoked potentials both in the auditory and the visual cortices (Wang et al., 2012, Amendola et al., 2014).

In conclusion, *Foxg1*haploinsufficiency causes a severe impairment in visual function that is likely due to altered cortical mechanisms. This should be taken into account when *Foxg1*$^{+/Cre}$ mice are used in behavioral experiments and when visual function is evaluated in patients carrying *FOXG1* mutations.

Acknowledgments

The work was partially funded by Telethon grant (GGP09117) and by Italian Health Ministry "Ricerca finalizzata 2010" (RF-2010-2317597) grant to AR. ES is recipient of a grant from Macula Vision Research Foundation.

References

Amendola E, Zhan Y, Mattucci C, Castroflorio E, Calcagno E, Fuchs C, Lonetti G, Silingardi D, Vyssotski AL, Farley D, Ciani E, Pizzorusso T, Giustetto M, Gross CT (2014) Mapping pathological phenotypes in a mouse model of CDKL5 disorder. PLoS One 9:e91613.

Ariani F, Hayek G, Rondinella D, Artuso R, Mencarelli MA, Spanhol-Rosseto A, Pollazzon M, Buoni S, Spiga O, Ricciardi S, Meloni I, Longo I, Mari F, Broccoli V, Zappella M, Renieri A (2008) FOXG1 is responsible for the congenital variant of Rett syndrome. American journal of human genetics 83:89-93.

Bahi-Buisson N, Nectoux J, Girard B, Van Esch H, De Ravel T, Boddaert N, Plouin P, Rio M, Fichou Y, Chelly J, Bienvenu T (2010) Revisiting the phenotype associated with FOXG1 mutations: two novel cases of congenital Rett variant. Neurogenetics 11:241-249.

Barone I, Novelli E, Piano I, Gargini C, Strettoi E (2012) Environmental enrichment extends photoreceptor survival and visual function in a mouse model of retinitis pigmentosa. PLoS One 7:e50726.

Belichenko PV, Wright EE, Belichenko NP, Masliah E, Li HH, Mobley WC, Francke U (2009) Widespread changes in dendritic and axonal morphology in Mecp2-mutant mouse models of Rett syndrome: evidence for disruption of neuronal networks. J Comp Neurol 514:240-258.

Brunetti-Pierri N, Paciorkowski AR, Ciccone R, Della Mina E, Bonaglia MC, Borgatti R, Schaaf CP, Sutton VR, Xia Z, Jelluma N, Ruivenkamp C, Bertrand M, de Ravel TJ, Jayakar P, Belli S, Rocchetti K, Pantaleoni C, D'Arrigo S, Hughes J, Cheung SW, Zuffardi O, Stankiewicz P (2011) Duplications of FOXG1 in 14q12 are associated with developmental epilepsy, mental retardation, and severe speech impairment. Eur J Hum Genet 19:102-107.

Castano G, Lyons CJ, Jan JE, Connolly M (2000) Cortical visual impairment in children with infantile spasms. J AAPOS 4:175-178.

Celesia GG (1982) Steady-state and transient visual evoked potentials in clinical practice. Annals of the New York Academy of Sciences 388:290-307.

Chen Q, Zhu YC, Yu J, Miao S, Zheng J, Xu L, Zhou Y, Li D, Zhang C, Tao J, Xiong ZQ (2010) CDKL5, a protein associated with rett syndrome, regulates neuronal morphogenesis via Rac1 signaling. J Neurosci 30:12777-12786.

Damiani D, Novelli E, Mazzoni F, Strettoi E (2012) Undersized dendritic arborizations in retinal ganglion cells of the rd1 mutant mouse: a paradigm of early onset photoreceptor degeneration. J Comp Neurol 520:1406-1423.

Dani VS, Chang Q, Maffei A, Turrigiano GG, Jaenisch R, Nelson SB (2005) Reduced cortical activity due to a shift in the balance between excitation and inhibition in a mouse model of Rett syndrome. Proc Natl Acad Sci U S A 102:12560-12565.

Dastidar SG, Bardai FH, Ma C, Price V, Rawat V, Verma P, Narayanan V, D'Mello SR (2012) Isoform-specific toxicity of Mecp2 in postmitotic neurons: suppression of neurotoxicity by FoxG1. The Journal of neuroscience : the official journal of the Society for Neuroscience 32:2846-2855.

De Filippis R, Pancrazi L, Bjorgo K, Rosseto A, Kleefstra T, Grillo E, Panighini A, Cardarelli F, Meloni I, Ariani F, Mencarelli MA, Hayek J, Renieri A, Costa M, Mari F (2012) Expanding the phenotype associated with FOXG1 mutations and in vivo FoxG1 chromatin-binding dynamics. Clin Genet 82:395-403.

de Freitas Dotto P, Cavascan NN, Berezovsky A, Sacai PY, Rocha DM, Pereira JM, Salomao SR (2014) Sweep visually evoked potentials and visual findings in children with West syndrome. Eur J Paediatr Neurol 18:201-210.

Della Sala G, Putignano E, Chelini G, Melani R, Calcagno E, Michele Ratto G, Amendola E, Gross CT, Giustetto M, Pizzorusso T (2015) Dendritic Spine Instability in a Mouse Model of CDKL5 Disorder Is Rescued by Insulin-like Growth Factor 1. Biological psychiatry.

Dineen J, Keating EG (1981) The primate visual system after bilateral removal of striate cortex. Survival of complex pattern vision. Exp Brain Res 41:338-345.

Duggan CD, DeMaria S, Baudhuin A, Stafford D, Ngai J (2008) Foxg1 is required for development of the vertebrate olfactory system. J Neurosci 28:5229-5239.

Durand S, Patrizi A, Quast KB, Hachigian L, Pavlyuk R, Saxena A, Carninci P, Hensch TK, Fagiolini M (2012) NMDA receptor regulation prevents regression of visual cortical function in the absence of Mecp2. Neuron 76:1078-1090.

Eagleson KL, Schlueter McFadyen-Ketchum LJ, Ahrens ET, Mills PH, Does MD, Nickols J, Levitt P (2007) Disruption of Foxg1 expression by knock-in of cre recombinase: effects on the development of the mouse telencephalon. Neuroscience 148:385-399.

Fiala JC, Spacek J, Harris KM (2002) Dendritic spine pathology: cause or consequence of neurological disorders? Brain Res Brain Res Rev 39:29-54.
Gan WB, Grutzendler J, Wong WT, Wong RO, Lichtman JW (2000) Multicolor "DiOlistic" labeling of the nervous system using lipophilic dye combinations. Neuron 27:219-225.
Guerrini R, Parrini E (2012) Epilepsy in Rett syndrome, and CDKL5- and FOXG1-gene-related encephalopathies. Epilepsia 53:2067-2078.
Hebert JM, McConnell SK (2000) Targeting of cre to the Foxg1 (BF-1) locus mediates loxP recombination in the telencephalon and other developing head structures. Developmental biology 222:296-306.
Jeon CJ, Strettoi E, Masland RH (1998) The major cell populations of the mouse retina. J Neurosci 18:8936-8946.
Krishnan K, Wang BS, Lu J, Wang L, Maffei A, Cang J, Huang ZJ (2015) MeCP2 regulates the timing of critical period plasticity that shapes functional connectivity in primary visual cortex. Proceedings of the National Academy of Sciences of the United States of America 112:E4782-4791.
Landi S, Putignano E, Boggio EM, Giustetto M, Pizzorusso T, Ratto GM (2011) The short-time structural plasticity of dendritic spines is altered in a model of Rett syndrome. Sci Rep 1:45.
Le Guen T, Bahi-Buisson N, Nectoux J, Boddaert N, Fichou Y, Diebold B, Desguerre I, Raqbi F, Daire VC, Chelly J, Bienvenu T (2011a) A FOXG1 mutation in a boy with congenital variant of Rett syndrome. Neurogenetics 12:1-8.
Le Guen T, Fichou Y, Nectoux J, Bahi-Buisson N, Rivier F, Boddaert N, Diebold B, Heron D, Chelly J, Bienvenu T (2011b) A missense mutation within the fork-head domain of the forkhead box G1 Gene (FOXG1) affects its nuclear localization. Hum Mutat 32:E2026-2035.
LeBlanc JJ, DeGregorio G, Centofante E, Vogel-Farley VK, Barnes K, Kaufmann WE, Fagiolini M, Nelson CA (2015) Visual evoked potentials detect cortical processing deficits in Rett syndrome. Ann Neurol 78:775-786.
Lenassi E, Likar K, Stirn-Kranjc B, Brecelj J (2008) VEP maturation and visual acuity in infants and preschool children. Doc Ophthalmol 117:111-120.
Lonetti G, Angelucci A, Morando L, Boggio EM, Giustetto M, Pizzorusso T (2010) Early environmental enrichment moderates the behavioral and synaptic phenotype of MeCP2 null mice. Biol Psychiatry 67:657-665.
Mariani J, Coppola G, Zhang P, Abyzov A, Provini L, Tomasini L, Amenduni M, Szekely A, Palejev D, Wilson M, Gerstein M, Grigorenko EL, Chawarska K, Pelphrey KA, Howe JR, Vaccarino FM (2015) FOXG1-Dependent Dysregulation of GABA/Glutamate Neuron Differentiation in Autism Spectrum Disorders. Cell 162:375-390.
Mencarelli MA, Spanhol-Rosseto A, Artuso R, Rondinella D, De Filippis R, Bahi-Buisson N, Nectoux J, Rubinsztajn R, Bienvenu T, Moncla A, Chabrol B, Villard L, Krumina Z, Armstrong J, Roche A, Pineda M, Gak E, Mari F, Ariani F, Renieri A (2010) Novel FOXG1 mutations associated with the congenital variant of Rett syndrome. J Med Genet 47:49-53.
Pancrazi L, Di Benedetto G, Colombaioni L, Della Sala G, Testa G, Olimpico F, Reyes A, Zeviani M, Pozzan T, Costa M (2015) Foxg1 localizes to mitochondria and coordinates cell differentiation and bioenergetics. Proc Natl Acad Sci U S A 112:13910-13915.
Patriarchi T, Amabile S, Frullanti E, Landucci E, Lo Rizzo C, Ariani F, Costa M, Olimpico F, J WH, F MV, Renieri A, Meloni I (2015) Imbalance of excitatory/inhibitory synaptic protein expression in iPSC-derived neurons from FOXG1 patients and in foxg1 mice. Eur J Hum Genet.
Pauley S, Lai E, Fritzsch B (2006) Foxg1 is required for morphogenesis and histogenesis of the mammalian inner ear. Dev Dyn 235:2470-2482.

Philippe C, Amsallem D, Francannet C, Lambert L, Saunier A, Verneau F, Jonveaux P (2010) Phenotypic variability in Rett syndrome associated with FOXG1 mutations in females. J Med Genet 47:59-65.
Porciatti V, Pizzorusso T, Maffei L (1999) The visual physiology of the wild type mouse determined with pattern VEPs. Vision Res 39:3071-3081.
Pratt T, Tian NM, Simpson TI, Mason JO, Price DJ (2004) The winged helix transcription factor Foxg1 facilitates retinal ganglion cell axon crossing of the ventral midline in the mouse. Development 131:3773-3784.
Rodriguez AR, de Sevilla Muller LP, Brecha NC (2014) The RNA binding protein RBPMS is a selective marker of ganglion cells in the mammalian retina. The Journal of comparative neurology 522:1411-1443.
Shen L, Nam HS, Song P, Moore H, Anderson SA (2006) FoxG1 haploinsufficiency results in impaired neurogenesis in the postnatal hippocampus and contextual memory deficits. Hippocampus 16:875-890.
Shoichet SA, Kunde SA, Viertel P, Schell-Apacik C, von Voss H, Tommerup N, Ropers HH, Kalscheuer VM (2005) Haploinsufficiency of novel FOXG1B variants in a patient with severe mental retardation, brain malformations and microcephaly. Hum Genet 117:536-544.
Siegenthaler JA, Tremper-Wells BA, Miller MW (2008) Foxg1 haploinsufficiency reduces the population of cortical intermediate progenitor cells: effect of increased p21 expression. Cereb Cortex 18:1865-1875.
Striano P, Paravidino R, Sicca F, Chiurazzi P, Gimelli S, Coppola A, Robbiano A, Traverso M, Pintaudi M, Giovannini S, Operto F, Vigliano P, Granata T, Coppola G, Romeo A, Specchio N, Giordano L, Osborne LR, Gimelli G, Minetti C, Zara F (2011) West syndrome associated with 14q12 duplications harboring FOXG1. Neurology 76:1600-1602.
Tian NM, Pratt T, Price DJ (2008) Foxg1 regulates retinal axon pathfinding by repressing an ipsilateral program in nasal retina and by causing optic chiasm cells to exert a net axonal growth-promoting activity. Development 135:4081-4089.
Tohyama J, Yamamoto T, Hosoki K, Nagasaki K, Akasaka N, Ohashi T, Kobayashi Y, Saitoh S (2011) West syndrome associated with mosaic duplication of FOXG1 in a patient with maternal uniparental disomy of chromosome 14. Am J Med Genet A 155A:2584-2588.
tom Dieck S, Brandstatter JH (2006) Ribbon synapses of the retina. Cell and tissue research 326:339-346.
Tomassy GS, Morello N, Calcagno E, Giustetto M (2014) Developmental abnormalities of cortical interneurons precede symptoms onset in a mouse model of Rett syndrome. Journal of neurochemistry 131:115-127.
Tropea D, Van Wart A, Sur M (2009) Molecular mechanisms of experience-dependent plasticity in visual cortex. Philosophical transactions of the Royal Society of London Series B, Biological sciences 364:341-355.
Wang IT, Allen M, Goffin D, Zhu X, Fairless AH, Brodkin ES, Siegel SJ, Marsh ED, Blendy JA, Zhou Z (2012) Loss of CDKL5 disrupts kinome profile and event-related potentials leading to autistic-like phenotypes in mice. Proc Natl Acad Sci U S A 109:21516-21521.
Wassle H, Puller C, Muller F, Haverkamp S (2009) Cone contacts, mosaics, and territories of bipolar cells in the mouse retina. J Neurosci 29:106-117.
Weiskrantz L (2009) Is blindsight just degraded normal vision? Exp Brain Res 192:413-416.
Williams RW, Strom RC, Goldowitz D (1998) Natural variation in neuron number in mice is linked to a major quantitative trait locus on Chr 11. The Journal of neuroscience : the official journal of the Society for Neuroscience 18:138-146.
Xiang M, Zhou L, Peng YW, Eddy RL, Shows TB, Nathans J (1993) Brn-3b: a POU domain gene expressed in a subset of retinal ganglion cells. Neuron 11:689-701.
Xuan S, Baptista CA, Balas G, Tao W, Soares VC, Lai E (1995) Winged helix transcription factor BF-1 is essential for the development of the cerebral hemispheres. Neuron 14:1141-1152.

The authors wish it to be known that, in their opinion, the first two authors should be regarded as joint First Authors.

Legend to Figures

Figure 1. Visual acuity in *Foxg1*$^{+/Cre}$ mice and wild-type littermates

(*A*) Examples of VEP waveforms recorded in response to 0.1 c/deg gratings. *(B)* VEP amplitude changes in response to gratings of high contrast and of decreasing bar size (increasing spatial frequency) in a wild-type (WT) and a *Foxg1*$^{+/Cre}$ mouse. VEP amplitude decreases by progressively increasing the spatial frequency. Visual acuity was determined by linearly extrapolating VEP amplitude to 0 V. Symbols represent data average data from all animals (WT n=9; *Foxg1*$^{+/Cre}$ *n*=5). Arrows in the abscissa point to visual acuity value. Dotted line represents average noise level. *(C)* Spatial resolution in the visual cortex of wild-type and *Foxg1*$^{+/Cre}$ mice. Visual acuity is significantly reduced in *Foxg1*$^{+/Cre}$ mice compared with wild-type littermates (*Foxg1*$^{+/Cre}$, 0.20 cycle/degree SEM 0.05, n=9; WT, 0.51 cycle/degree, SEM 0.05 n=5; *****, *P*,0.01, Student's *t* test).

Figure 2. Retinal morphology in *Foxg1*$^{+/Cre}$ animals and wild-type littermates

Retinal morphology in *Foxg1*$^{+/Cre}$ (A and C) and wt (B and D) mice. A, B: Low magnification images of retinal sections stained with rhodopsin antibodies (green signal), showing normal retinal laminations and bright staining of photoreceptor outer segments (OS) in both mutant and wt mice. Red: nuclear counterstaining. In A the normal morphology of the optic nerve head (ONH) can be appreciated. The insets show at 2x details of photoreceptor rows and outer segments. Here and in the following images: ONL, IPL outer nuclear and inner plexiform layer, respectively. C and D: examples of retinal ganglion cells (GC) stained by the type specific transcription factor Brn3-B (red), with nuclear localization, and by neurofilament antibodies (green), depicting their morphology in detail.

Figure 3. M**orphology of neuronal subtypes in *Foxg1*$^{+/Cre}$ mice and wild-type littermates**

Morphology of retinal neuronal subtypes in *Foxg1*$^{+/Cre}$ (left panels) and wt mice

Retinal neurons in *Foxg1*$^{+/Cre}$ (left panels) and wt mice. A, B: rod bipolar cells have been labelled red by PKC antibodies. Their dendrites form dense plexa in the OPL while axonal endings (rbe) cluster in regularly in the deepest part of the IPL. Green puncta are synaptic ribbons from glutamatergic processes, regularly arranged in the two plexiform layers. Blue: nuclearcounterstaining. C,D: types of cone bipolar cells stained by ZnP-1 (synaptotagmin antibodies). Both dendritic tips in the OPL and axonal arbors in the IPL have the expected fine structure. The IPL show three typical bands, revealed by calretinin staining of amacrine cells (red). E, F: Cholinergic amacrine cells, stained red by ChAT antibodies, are arranged in two mirror-

symmetric populations at the two margins of the IPL. Alpha-like ganglion cells, labelled by SMI-32 antibodies (green) have well preserved morphologies in both mutant and wt retinas.

Fig.4. Neurons in the GCL of *Foxg1*$^{+/+}$ and *Foxg1*$^{+/Cre}$ mice

A,B. Cells in the GCL have been labelled by antibodies against the RNA binding protein RBPMS that produce a cytoplasmic staining in GCs selectively (green signal). Ethidium counterstaining (red signal) show the nuclei of GCs and displaced amacrine cells (AC).The general morphology (A and B) and the total number of cells in the GC layer (C) are virtually identical in *Foxg1*$^{+/+}$ (A) and *Foxg1*$^{+/Cre}$ (B) mice. Quantification in C. The number of GCs proper (D) is also not different between the two strains (D).

Figure 5. Immunohistochemistry on visual cortex of *Foxg1*$^{+/+}$ and *Foxg1*$^{+/Cre}$ mice

Panel A. A significant reduction of NeuN staining is present in layer II-III and IV of the visual cortex of Foxg1$^{+/Cre}$ mice (WT: n=4; *Foxg1*$^{+/Cre}$= n=4; two-ways RM ANOVA genotype X cortical layer p=0.003; post-hoc Sidak wt vs. *Foxg1*$^{+/Cre}$ within layer II-III p=0.004, within layer IV p=0.006).

Panel B. Calretinin positive cells in visual cortices from WT and *Foxg1*$^{+/Cre}$ mice. Quantification of calretinin positive cells density in visual cortical layers of WT and *Foxg1*$^{+/Cre}$ mice shows a significant increase of calretinin positive cells in layer II-III and VI of the *Foxg1*$^{+/Cre}$ cortex (two-ways RM ANOVA genotype X cortical layer p=0.04; post-hoc Sidak wt vs. *Foxg1*$^{+/Cre}$ within layer II-III $p<0.01$, within layer VI $p<0.05$).

Panel C Parvalbumin positive cells in visual cortices from WT and *Foxg1*$^{+/Cre}$ mice. Quantification of parvalbumin positive cells density in visual cortical layers of WT and *Foxg1*$^{+/Cre}$ mice shows a significant decrease of parvalbumin positive cells in layer II-III of the *Foxg1*$^{+/Cre}$ cortex (two-ways RM ANOVA genotype X cortical layer p=0.03; post-hoc Sidak wt vs. *Foxg1*$^{+/Cre}$ within layer II-III $p<0.01$).

Panel D GAD67 positive cells in visual cortices from WT and *Foxg1*$^{+/Cre}$ mice. Quantification of GAD67 positive cells density in visual cortical layers of WT and *Foxg1*$^{+/Cre}$ mice shows that the density of GAD67 positive cells is not statistically different between wt and *Foxg1*$^{+/Cre}$ mice (two-ways RM ANOVA effect of genotype p=0.44, genotype X cortical layer p=0.33)..*: $p<0.05$; **: $p<0.01$.

Figure 6. Dendritic spine length and density in *Foxg1*$^{+/Cre}$ animals and wild-type littermates

A) Confocal microscope images of WT and *Foxg1*$^{+/Cre}$dendritic segment. Scale bar= 5µm. B and C) Average dendritic spine length and density (respectively) in basal dendrites of layer 4/5 pyramidal cells of *Foxg1*$^{+/Cre}$and WT mice. A significant decrease in spine density was measured in *Foxg1*$^{+/Cre}$ as compared to wt mice (WT: n= 7; *Foxg1*$^{+/Cre}$: n=7; p=0.045, Student's *t* test).

*Manuscript with Highlighted or Tracked Changes
Click here to download Manuscript with Highlighted or Tracked Changes: Text Highl2016.docx Click here to view linked References

Visual impairment in *FOXG1*-mutated individuals and mice

Comment [M1]: term patient was replaced by subject or individual along the entire paper

Elena M Boggio[1,£,#], Laura Pancrazi [1,2#], Mariangela Gennaro [1,6], Caterina Lo Rizzo [3,4], Francesca Mari [3,4], Ilaria Meloni [3], Francesca Ariani [3,4], Anna Panighini[1], Elena Novelli [1],Martina Biagioni [1, 5], Enrica Strettoi [1], Joussef Hayek [7], Alessandra Rufa [5], Tommaso Pizzorusso [1,6*], Alessandra Renieri [3,4*] and Mario Costa [1,2]

1 CNR Neuroscience Institute, Pisa Italy

2 Scuola Normale Superiore, BioSNS lab, Pisa Italy

3 Medical Genetics, University of Siena, Siena, Italy

4 Genetica Medica, Azienda Ospedaliera Universitaria Senese, Siena, Italy

5 Tuscan Doctorate School, University of Firenze, Firenze, Italy

6 Eye Tracking and Visual Application Lab (EVAlab), University of Siena, Siena, Italy

7 NEUROFARBA Department, University of Firenze, Firenze, Italy

8 Child Neuropsychiatry Unit, University Hospital, AOUS, Siena, Italy

*Corresponding authors:

Tommaso Pizzorusso tommaso@in.cnr.it

Alessandra Renieri alessandra.renieri@unisi.it

# both authors equally contributed to the work

£ Current address: Dept of Veterinary Science, University of Turin

Abstract

The *Forkead Box G1* (*FOXG1*in humans, *Foxg1* in mice) gene encodes for a DNA−binding transcription factor, essential for the development of the telencephalon in mammalian forebrain. Mutations in *FOXG1* have been reported to be involved in the onset of Rett Syndrome, for which sequence alterations of *MECP2* and *CDKL5* are known. While visual alterations are not classical hallmarks of Rett syndrome, an increasing body of evidence shows visual impairment in patients and in *MeCP2*and *CDKL5* animal models. Herein we focused on the functional role of FOXG1 in the visual system of animal models (*Foxg1*$^{+/Cre}$ mice) and of a cohort of subjects carrying *FOXG1* mutations or deletions. Visual physiology of *Foxg1*$^{+/Cre}$ mice was assessed by visually evoked potentials, which revealed a significant reduction in response amplitude and visual acuity with respect to wild-type littermates. Morphological investigation showed abnormalities in the organization of excitatory/inhibitory circuits in the visual cortex. No alterations were observed in retinal structure. By examining a cohort of *FOXG1*-mutated individuals with a panel of neuro-ophthalmological assessments, we found that all of them exhibited visual alterations compatible with high level visual dysfunctions. In conclusion our data show that *Foxg1* haploinsufficiency results in an impairment of mouse and human visual cortical function.

Keywords: Rett syndrome, Autism, West syndrome, visual cortex, inhibitory interneurons, cortical blindness

Rett Syndrome (RTT) is a neurodevelopmental disorder representing one of the most common causes of intellectual disability in girls. Beside the classical form due to *MECP2* mutations, two other forms have been associated to specific molecular defects, namely the early-onset seizure variant, mostly due to *CDKL5* mutations, and the congenital variant, mostly due to *FOXG1* mutations. The association between the *FOXG1* gene (OMIM#164874) and the congenital variant of RTT is relatively recent (Ariani et al., 2008), and since its discovery an increasing number of patients with *FOXG1* point mutations have been reported. The human *FOXG1* gene is located in the 14q12 chromosome and encodes for a phylogenetically well conserved DNA-binding transcription factor of 489 aa. The mechanisms by which *FOXG1* mutations cause RTT are still unknown, however the presence of *FOXG1* on an autosomic chromosome suggests haploinsufficiency as a candidate for the aetio-pathological mechanisms of this RTT variant (Shoichet et al., 2005, De Filippis et al., 2012). Furthermore, a physical interaction between MeCP2 and FOXG1 has been demonstrated (Dastidar et al., 2012) suggesting that, at least in the Central Nervous system (CNS), an impairment in FOXG1-MeCP2 interaction could be critical for the development of RTT. Intriguingly, a recent report indicates that Foxg1 displays, together with a nuclear localization, a specific targeting to mitochondria. This finding sheds new light on the etiology of FOXG1-RTT and on the original mitochondrial dysfunction hypothesis for the RTT pathogenesis (Pancrazi et al., 2015).

Foxg1 presence is essential for the embryonic development of the telencephalon in mammalian forebrain (Xuan et al., 1995). Its expression is abundant since the early development, persisting at lower levels in the adult cortex including the visual areas (Shen et al., 2006). This pattern suggests that specific aspects of the RTT associated with *FOXG1* mutations might involve visual cortical circuits. Foxg1 is also necessary for the correct formation of the inner ear and the olfactory system (Pauley et al., 2006, Duggan et al., 2008) and the appropriate crossing of retinal ganglion cell axons during development (Pratt et al., 2004). Interestingly, recent data show that Foxg1 overexpression is associated with neurodevelopmental pathologies and autism (Mariani et al., 2015).

Foxg1 null mice were first obtained in 1995: while *Foxg1*$^{+/-}$ animals were believed to have a normal phenotype, *Foxg1*$^{-/-}$ mutants showed a dramatic reduction in the size of the cerebral hemispheres and died at birth. Due to the lethal phenotype, functional studies in null animals were initially restricted to the determination of the mechanisms influencing the forebrain size and the development of the telencephalon. More in depth analysis of the *Foxg1*$^{+/-}$ model showed microcephaly, hyperlocomotion, impaired habituation in the open field and a severe deficit in contextual fear conditioning, recapitulating some features of disorders derived from deregulation of

Comment [M2]: "Mental retardation" was replaced by "Intellectual disability" along the entire paper.

FOXG1 expression such as the congenital variant of RTT and West syndrome (Shen et al., 2006, Eagleson et al., 2007, Siegenthaler et al., 2008). These features suggested the possibility to use *Foxg1*$^{+/-}$ mutants as models for these diseases (Shen et al., 2006, Ariani et al., 2008, Bahi-Buisson et al., 2010, Mencarelli et al., 2010, Philippe et al., 2010, Le Guen et al., 2011a, Le Guen et al., 2011b, Striano et al., 2011, Tohyama et al., 2011).

Recent work showed that the visual system is altered in mouse models of RTT (Tropea et al., 2009, Durand et al., 2012, Krishnan et al., 2015) providing the opportunity to use the visual system to investigate the patho-physiology of RTT and to improve objective patient evaluation. Indeed, a specific cortical processing deficit has been discovered using pattern reversal VEPs in RTT patients. Importantly, amplitude and latency of VEP waveforms are related to disease stage, clinical severity and MECP2 mutation (LeBlanc et al., 2015). The hypothesis that *FOXG1* mutations affects visual development is also supported by data showing that in West syndrome patients, altered VEPs and poor visual behavior are hallmarks of the pathology (de Freitas Dotto et al., 2014). These data prompted us to analyze whether visual deficits were also present in Foxg1 RTT patients and in *Foxg1*$^{+/-}$mice. *FOXG1* subject's visual behavior suggested a high level visual dysfunction compatible with the blind-sight syndrome occurring in individuals with extensive damage of primary visual cortex and consisting in loss of awareness for visual stimuli. Similarly, mouse studies point to a severe alteration in the development of cortical inhibitory and excitatory circuits. The results of this study show that cortical visual impairments occur in both patients and animal model of RTT.

Experimental procedures

Subjects

FOXG1 subjects: Eight subjects (5 females and 3 males) with a *FOXG1* mutation were enrolled in the study. Age ranged from 9 months to 22 years (Table 1). All subjects had a clinical diagnosis of the congenital variant of RTT, with severe intellectual disability with early regression phase, severe microcephaly (range -3SD/-8SD) mostly postnatal, stereotypic handand tongue movements. One subject showed generalized epileptic seizures. Sleep disturbances were present in 5 out of 6 individuals in whom the information was collected. Brain MRI was available for 6 cases. It was typical in one while the other 5 showed corpus callosum agenesis or hypoplasia and other brain asymmetries (Table 1). Menstrual disorders are not reported in the only girlin post-pubertal age (patient 8).

Four subjects showed a 14q12 micro deletion involving the FOXG1 gene ranging in size from 1.1Mb to 6.73Mb; four showed a point mutation predicted to lead to a truncation of the protein (Table 1).

Controls were 20 subjects (10 males and 10 females, mean age 7.8 years; range12 months-22 years). None of them reported neurological problems, seizures, visual system diseases or history of pre- or perinatal illness. Subjects with refractive errors exceeding ± 1.5 diopters and strabismus were excluded. Regular neuro-ophthalmologic assessments were performed in each subject, including tests of visual acuity, color sensitivity, pupil reactivity, ocular alignment, fixation and motility, slit lamp evaluation, confrontation visual field testing, fundoscopy and recording of standard flash VEPs (Celesia, 1982, Lenassi et al., 2008).

1) Subjects ~~Patient~~ clinical assessment: Genetic counseling and clinical assessment were performed for 5 out of 8 subjects by the same clinical geneticists (AR and MF) and child neuropsychiatrist (JH). Clinical data of the remaining 3 patients were collected through clinical reports provided bythe families (patients 1,2,5).

2) Visual Assessment: Clinical neuro-ophthalmologic data of each subject, evaluated by an experienced neuro-ophthalmologist (AR),were collected, together with an extensive parents' interview, specificfor visual abilities impairment. Patients were approached gradually by planning several sections of examination or observation. The following visual tests were performed: refractive errors measurement (by cycloplegia and correction with appropriate lenses); an estimate of visual acuity and color vision (obtained using a modified form of forced choice-preferential

Comment [M3]: terms normal and abnormal were replaced by typical and atypical along the entire paper when refer t human subjects.

looking method); ocular alignment and fixation; oculo-cephalic reflexes; optokinetic nystagmus (when possible), cranial nerve examination; pupil reactivity evaluation; slit lamp examination; dilated fundoscopy. An estimation of visual field extension and subject's interest towards colored or familial stimuli compared to unfamiliar or non-colored stimuli was obtained during the examination; finally, visual engagement and visual-manual coordination were also evaluated. Brain MRI, EEG and flash VEP datawere collected whenever the examination was possible.

Animals

The Foxg1-cre line was created by replacing the intron-less Foxg1 coding region (expressed specifically in the telencephalic cells) with cre recombinase, resulting in a *Foxg1* heterozygous mouse with reduced expression of Foxg1 (Hebert and McConnell, 2000).
Foxg1$^{+/Cre}$ mice founders were a generous gift from Dr. Vania Broccoli. Animals were housed in a 12-h light/dark cycle with free access to food and water. All the experiments were carried out in accordance with the directives the European Community Council (86/609/EEC) and approved by the Italian Ministry of Health. All mice used in this study were generated by heterozygous wild type matings of the original *Foxg1*^{Cre}background (C57BL/6J) male with a wild type C57BL/6J female. This breeding scheme was used since the heterozygous animals show behavioral abnormalities in the parental care. C57BL/6J (wild type) mice were purchased from the Jackson Laboratories (Bar Harbor, ME, USA).

Statistics and data collection.

Data were collected and analyzed by investigators blind to the genetic and treatment status of the animal. Only animals with significantly altered EEG or breath rate during VEP recordings were discarded. Sample size was estimated by power analysis using data present in the literature on VEP and inhibitory circuit alterations in mouse models of neurodevelopmental disorders. Animals were randomly assigned to the various experimental groups caring that littermates were divided in the different experimental groups. To analyze data we used the paired t-test (to compare two repeated measures on the same subjects) and the t-test (to compare between different subjects). ANOVA was used to compare many groups. P=0.05 was assumed as significance level. Statistical analysis was performed using the Sigma Stat (Systat, USA) software.

Visually evoked potentials

Mice were anesthetized with an intraperitoneal injection of 20% urethane and mounted in a stereotaxic apparatus allowing a full view of the visual stimulus. After carefully removing a portion of the skull overlying the binocular visual cortex while leaving the dura mater intact, a glass-pulled recording electrode filled with NaCl (3 M) was inserted into the visual cortex perpendicularly to the stereotaxic plane. The electrode was inserted 100 µm deep from pial surface and 2.7-3 mm lateral in correspondence to lambda. The electrical signals were amplified (10,000-fold), band-pass filtered (0.3–100 Hz), digitized, and averaged (at least 75 events in blocks of 5 each). The transient VEPs in response to an abrupt contrast reversal (1 Hz) were evaluated by measuring the peak-to-trough amplitude. The visual stimuli consisted of horizontal gratings of different spatial frequencies and contrasts generated by a visual stimulator interface (VSG2:2 card; Cambridge Research System, Cheshire, UK) and presented on a monitor (Sony model CPD-G520) placed 20 cm in front of the animal.

Immunohistochemistry on visual cortex of *Foxg1*$^{+/+}$ and *Foxg1*$^{+/Cre}$ mice

Animals were deeply anaesthetized and perfused transcardially with PBS 1X followed by 4% paraformaldehyde. Brains were removed, post-fixed in the same fixative at 4°C and cryoprotected by immersion in 30% sucrose. Forty µm coronal sections were cut on a freezing microtome and processed for immunohistochemistry. Free floating sections were incubated for 1-2 hours in a blocking solution (10% BSA, 0,3% Triton X-100 in PBS), then in the primary antibody solution over night (O/N). The following day, the sections were incubated with appropriate secondary antibodies, mounted on glass slides and acquired with a Leica TCS-SP confocal microscope. The images were analyzed with ImageJ software. The following primary Abs were used: NeuN (1:500; Millipore, Billerica, MA, USA), MeCP2 (1:1000 cat. n. M 9317 Sigma Aldrich, Germany), parvalbumin (1:1000, Sigma Aldrich, Germany), calretinin (1:1000, Swant, Switzerland) and GAD67 (1:500, Chemicon, USA). Secondary antibodies used were Alexa Fluor 488 and Alexa Fluor 555 from Invitrogen.

Immunohistochemistry on retinal sections of *Foxg1*$^{+/+}$ and *Foxg1*$^{+/Cre}$ mice

Whole eyes were removed from deeply anesthetized mice (4 *Foxg1*$^{+/Cre}$ and 4 wt mice), cut at the ora serrata and fixed for 1 hr in 4% paraformaldehyde. The anterior segments were removed, the eye cups rinsed in 0.1M phosphate buffer (PB), cryoprotected in 30% sucrose, infiltrated in OCT and snap frozen in isopentane/dry ice. Afterwards, the eye cups were sectioned vertically at 12 µm on a Leica cryostat. The sections were collected on coated slides, processed for immunofluorescence using a panel of primary antibodies and reacted with appropriated secondary

antibodies conjugated with Alexa Fluor 488 (from Invitrogen), Rodamine RedX or Cy3 (from Jackson). Selected sections were counterstained with micromolar solutions of Ethidium homodimer-1 or BOBO 1-iodide nuclear dyes (from Invitrogen). All preparations were screened with a Zeiss Axioplan microscope equipped with a colorAxioplan camera. Selected sections were imaged at high resolution by confocal microscopy or with a Zeiss Apotome apparatus. The following antibodies were used: for photoreceptors: rhodopsin (RET-P1Sigma #O4886) and cone-specific L and M opsins (Millipore #AB5404 and #AB5407); for rod bipolar cells: PKCα (Sigma #P4334);for selected cone bipolar cell types: synaptotagmin2 - ZNP1 (ZIRC, Zebrafish International Resource Center); for amacrine cells:calretinin (Swant #7699/4); for cholinergic amacrine cells:ChAT (Chemicon #AB114P); for horizontal and ganglion cells:Neurofilament 200 (Sigma #N0142); for ganglion cells: SMI-32 (Covance#SMI32R) and Brn3 (Santa Cruz sc-6026); for synaptic ribbons: CtBP2 (Ribeye, BD Transduction Lab. #612044);for mitochondria: SOD2 (Invitrogen#A21990).

Counts of cells in the ganglion cell layer (GCL)

Additional *Foxg1*$^{+/+}$ and *Foxg1*$^{+/Cre}$ mice were used for counting cells in the ganglion cell layer (GCL) following published protocols (Damiani et al., 2012, Rodriguez et al., 2014). Briefly, paraformaldheyde fixed retinas (n=3 per strain, each from a different animal) were isolated from eye cups, the vitreous removed and 4 partial cuts made to delimitate the dorsal, nasal, ventral and temporal quadrants. After washes in 0.01M PBS, the retinas were blocked overnight at 4°C in a solution containing 0.5% Triton X-100 and 5% goat serum. Then, they were incubated for 6 days at 4°C with an anti-RNA binding protein (RBPMS), guinea pig antibody (Phospho_Solutions, CO, USA), specific for GCs (diluted 1:500), with 1% serum and 0.1% Triton X-100. After 3x20' washing in PBS, the retinas were incubated in Alexa Fluor 488-conjugated goat anti-guinea pig secondary antibody (Vector Laboratories, Burlingame, CA) diluted 1:800, washed 3x20' in PBS and counterstained for 2 hrs with Ethidium homodimer 1 (Vector Laboratories), diluted 1:1,000. After washing, retinal samples were finally mounted "ganglion cells up" in Vectashield. Retinal profiles of whole mount preparations were imaged in bright field with an Axiocam camera attached to a Zeiss microscope, using a 1.25x objective. Retinal areas were then measured on image tiff files using the edge detector tool of a Metamorph® routine. Flat-mounted retinas were imaged with a Zeiss Apotome fluorescence microscope using a 40x/1.5 n.a. Plan Neofluar oil objective. Five focal series of images (each covering a retinal area of 224 x 168 µm) were acquired in each of the four retinal quadrants at regular intervals from the periphery towards the optic nerve head. Serial optical sections (10-20), 0.5 µm apart, covering the thickness of the GCL were obtained. Projection images

Formatted: Highlight

Formatted: Highlight

were than generated and used for counting separately RBPMS positive cells (labelled green) and the nuclei of all the neurons in the layer, (labelled red), and comprising also those of displaced amacrine cells. The nuclei of blood vessel cells were excluded based on their typical elongated shape, small size and high brightness. Serial optical sections were used to count cells by navigating through z-stacks of the GCL in central retina areas characterized by elevated cell density.Total numbers of cells per retina were obtained multiplying average cellular densities by corresponding retinal areas.

Dendritic spine analysis.

Animals (n=3 for each genotype) were deeply anesthetized and perfused through the heart with 4% paraformaldehyde. A block of visual cortex was sectioned in the coronal plane into 300-µm-thick slices by using a vibratome. The lipophilic dye 1,1′-dioctadecyl-3,3,3′,3-tetramethylindocarbocyanine (DiI) (Invitrogen) was coated onto tungsten particles (diameter 1.1 µm; Bio-Rad) according to Gan et al. (Gan et al., 2000). DiI-coated particles were delivered to the slices by using a Helios Gene Gun System (Bio-Rad). A polycarbonate filter with a 3.0-µm pore size (Molecular Probes) was inserted between the gun and the preparation on a platform to remove clusters of large particles. Density of labeling was controlled by gas pressure (80 psi of helium). After labeling, slices were fixed in 4% paraformaldehyde. Labeled structures were analyzed by confocal microscopy. Images of basal dendrites of layer 2/3 pyramidal cells were acquired, stacked (0.5 µm step), and then analyzed with ImageJ. A total of 49 cells were counted; at least 6 dendrites per neuron were analyzed for a total number of 8820 spines. We measured the average spine lengths and densities (number of spines per length of dendrite) for each animal and calculated the mean per group.

Results

Visual performance in control subjects

All subjects with age older than 4 years showed a best corrected visual acuity between 20/20-20/25, color vision was 15/15 (Hishihara platelets), pupils were reactive, anterior segment and lenses were clear, fixation was stable and ocular motility was normal. Younger patients (age under 4 years) showed a good engagement for near and far visual stimuli, they were able to follow light and objects and were also able to reach or grasp objects of interest even if presented in a crowded surrounding. VEPs results in control subjects showed a mean latency of the P100 of 99.19 ms(range 90-105 ms); and a mean amplitude of the N75-P100 of 7,37 µV(range 5-10,1 µV).

Visual impairment in patients with *FOXG1* mutations

Considering that West syndrome patients carrying unbalanced levels of FOXG1 show visual impairment and that RTT models show abnormal development and plasticity of the visual system (LeBlanc et al., 2015), we decided to investigate whether patients with FOXG1 mutations displayed visual atypicalities (Castano et al., 2000). In all patients (Table 1), visual attention and engagement worsened with fatigue both when observed during examination and as reported by parents. Patients were apparently receptive to near (within reaching) visual stimuli that captured their attention. Actually, bright colored stimuli and moving objects (particularly when presented at short distance) were preferred. Patients' attention and awareness strongly decreased for far visual stimuli particularly when they were assembled with other objects (crowded surrounding). In these conditions, acoustic stimuli favored a brief visual engagement. Four patients out of eight demonstrated an inconstant ability to recognize familial faces (essentially parents), as observed during examination and reported by parents (Table 1). All patients had a variable dissociation between looking and reaching and demonstrated reduced or absent visual contact. All patients except one (#7) showed scarce visual engagement and no voluntary gazing toward surrounding visual stimuli. However, they were able to avoid obstacles or had a reaction of defense. They also showed an asymmetrical refractive defect between the two eyes. Four out of eight patients were photophobic and one showed compulsive gazing to bright light (#5). Anterior segment was typical in all patients. Pupils were reactive in seven out of eight cases. A jerk nystagmus was present in one patient (#2). Variable degrees of eyes misalignment and strabismus (exo and esotropia) were previously diagnosed in all patients. One patient presented a congenital oculomandibular syncinesia (#3). At fundoscopy, three patients showed smaller shape but typical appearing optic discs. Flash

Field Code Changed

VEPs, performed in three out of eight patients, were in the range of controls (see table 1). EEG showed epileptic changes particularly in occipital parietal and temporal parietal regions in two patients. These data prompted us to further characterize visual impairment and uncover the underlying neural defects exploiting a mouse model of *Foxg1* haploinsufficiency.

Reduced cortical VEP acuity in *Foxg1*$^{+/-}$ Mice.

To investigate possible consequences of the Foxg1 haploinsufficiency on visual function, we analyzed visual responses by recording Visually Evoked Potentials (VEP), a well-established technique for measuring overall visual function in mammals (Porciatti et al., 1999). Three Foxg1 heterozygous models (*Foxg1*$^{+/tet}$, *Foxg1*$^{+/lacZ}$ and *Foxg1*$^{+/cre}$) showing similar phenotype have been described in the literature (Shen et al., 2006, Eagleson et al., 2007). Among them, we choose the widely used *Foxg1*$^{+/Cre}$ mice on a C57/BL6J background, which shows the most evident anatomical alterations of the cerebral cortex (Eagleson et al., 2007). Heterozygous mice were chosen because they better recapitulate the patient condition, insofar homozygous animals show birth lethality and a dramatic reduction in the size of the cerebral hemispheres.
As expected, VEP responses to alternating gratings decreased in amplitude in response to increments of the spatial frequency of the stimulus (Fig. 1). As shown in Fig. 1A, VEP transient amplitude is plotted against the spatial frequency log and visual acuity is taken as the spatial frequency that coincides with the extrapolation to zero amplitude of the linear regression. Visual acuity was significantly reduced in P30 *Foxg1*$^{+/Cre}$ mice compared to wild-type littermates (*Foxg1*$^{+/Cre}$, 0.20 +/- 0.05 cycles/degree, n=9; WT, 0.51 cycles/degree, n=5; *, P=0.01, t-test, Fig. 1B). Moreover, VEP amplitudes at low spatial frequency were strongly diminished in *Foxg1*$^{+/Cre}$ mice (0.1 c/deg, wt 166.3 μV SEM 18.1, *Foxg1*$^{+/Cre}$ 18.1 μV SEM4.6; t-test, p<0.001). These data suggest that FOXG1 mutations could result in visual impairments in mice as in humans.

Retinal morphology in *Foxg1*$^{+/Cre}$ and wt mice.

To assess whether *Foxg1* haploinsufficiency results into evident abnormalities in retinal morphological organization, we probed retinal sections of *Foxg1*$^{+/Cre}$ mice and wild type littermates (n=3 per mice, per strain) with a panel of antibodies, comprising well established cell-type specific markers, indicators of retinal lamination and constituents of retinal synaptic contacts (Jeon et al., 1998, tom Dieck and Brandstatter, 2006, Wassle et al., 2009, Barone et al., 2012).

Retinal neurons of all the five classes (photoreceptors, horizontal, bipolar, amacrine and ganglion cells), were labeled and compared among the two strains (Fig. 2, 3). None of the used retinal markers revealed obvious differences in the thickness of retinal layers, in their lamination pattern or in the morphology of individual cell types, between mutant and wt mice. Rhodopsin antibodies and ethidium nuclear staining highlighted a regular array of rod photoreceptors with no signs of degeneration (Fig.2, A-B). Cones displayed the normal, elongated morphology with outer segments of adequate length and orientation. Similarly, the main neurons of the retino-fugal ("vertical") pathway, and namely rod bipolars (Fig. 3, A-B) and types of cone bipolars belonging to the "On" and "Off" functional varieties (C, D), had well ramified dendrites; their axonal arbors terminated in the appropriate sublaminae of the inner plexiform layer. Cholinergic processes, constituted by the dendrites of starburst amacrine cells, retained the characteristic distribution in two parallel bands precisely located at 1/3 and 2/3 of the inner plexiform layer (Fig.3, E and F). Calretinin staining revealed a third tier of processes, regularly positioned between the two cholinergic bands (Fig. 3, C and D). Ribeye, a marker of ribbons at retinal glutamatergic synapses (established by photoreceptors and bipolar cells) had the expected distribution in the outer and inner retina (Figure 3, A and B). Particular attention was paid to the analysis of the morphology and the number of ganglion cells (GCs), known to display abnormalities in axonal projections in homozygous mice (Pratt et al., 2004, Tian et al., 2008). SMI-32 anti-neurofilament antibodies highlighted a tier of large-size cell bodies corresponding to alpha-like ganglion cells, while immunolabeling for Brn3B, the transcription factor selectively expressed in these neurons (Xiang et al., 1993) showed a similar pattern of nuclear staining in the ganglion cell layer (GCL) of mutant and control retinas (Fig.2 C-D). Similarly, immunostaining with 200 kDa neurofilament antibodies showed a regular arrangement of cell bodies in theGCL, the expected bundles of axons in the optic fiber layer and profuse dendritic ramifications in the inner plexiform layer (Fig.3, E-F).The morphology of the optic nerve head in mutant mice appeared normal as well (Fig.2 A).

The GCL contains amacrine and ganglion cells, approximately in equal number in the rodent retina. Cell counts of retinal whole mounts (Fig. 4) from *Foxg1*$^{+/Cre}$ (n=3 retinas) and *Foxg1*$^{+/+}$ (wt) mice (n=3) demonstrated that the two strains did not differ in the absolute number of cells in the GCL (*Foxg1*$^{+/Cre}$ 106300, SEM 5369; *Foxg1*$^{+/+}$115475 cells SEM 4803, t-test; p=0.27; Fig.4 A-C). Selective counts of GCs, labeled with a RBPMS cell type-specific antibody, showed overlapping numbers of these neurons in mutant and wt strains (Fig.4 D). Noticeably, the numbers obtained here are not different from previously published data accounting for the total number of cells in the GCL (Jeon et al., 1998) and of GCs (Williams et al., 1998) of C57Bl6 mice.

In conclusion, no changes in general organization, architecture and pattern of lamination were observed in retinas of *Foxg1*$^{+/Cre}$ mice, which appeared undistinguishable from those of their wt littermates. The heterozygous expression of FoxG1 does not affect the total number of cells in the innermost retinal layer.

Morphological analysis of the visual cortex of *Foxg1*$^{+/Cre}$ mice.

Prompted by the strong functional impairment in cortical VEPs, we investigated the architecture of excitatory and inhibitory neurons in the visual cortex of *Foxg1* haploinsufficient mice.

As a general neuronal marker, we assessed the pattern of Neu-N immunostaining in P30 *Foxg1*$^{+/Cre}$ mice. As already reported (Eagleson et al., 2007), the visual cortex is thinner in this line of mutants.(wt 914.3 µm SEM 12.6; *Foxg1*$^{+/Cre}$ 747.9 µm SEM 29.8; n=4 for each group, t-test p=0.002). To determine the occurrence of layer-specific effects of *Foxg*1 haploinsufficiency on neuronal density, we quantified Neu-N positive neurons along the cortical depth. As shown in Fig. 5A, a significant reduction specific for layer II-III and layer IV was found in the mutant mice as compared to wt littermates.

To assess whether morphological defects were associated with specific neuronal populations, we first studied markers of inhibitory interneurons since disruption in interneuron circuits has been found in RTT mouse models (Durand et al., 2012, Tomassy et al., 2014, Krishnan et al., 2015), and then we investigated alterations in dendritic spines of excitatory pyramidal cells.

Calretinin (CR), parvalbumin (PV) and GAD67 immunostaining. Since maturation of cortical inhibition in visual areas is correlated with maturation of visual acuity and defects in cortical inhibition have been found in other mouse models of RTT (Dani et al., 2005, Lonetti et al., 2010), we decided to investigate the number of cortical inhibitory cells in *Foxg1*$^{+/Cre}$ mice. Therefore, we estimated the density of CR, PVand GAD67 positive cells in the visual cortex at P30. CR immunostaining highlighted a significant increase in the interneuron density in the layers II-III and VI of the *Foxg1*$^{+/Cre}$ cortex with respect to wt (Fig. 5B). By contrast, we observed a reduction of PV positive cell density in layers II-III of the visual cortex (Fig. 5C). The total number of inhibitory cells calculated using GAD67 immunohistochemistry was not affected in heterozygous *Foxg1*$^{+/Cre}$ mice (Fig. 5D).

Dendritic spine density and length. Alterations in density and size of dendritic spines have been found in *Mecp2* mouse models of Rett Syndrome (Belichenko et al., 2009, Landi et al., 2011) and

also in many other models of neurodevelopmental disorders (Fiala et al., 2002). To investigate morphological alterations induced by Foxg1 haploinsufficiency, we evaluated by diolistic labeling the spine density and length in the basal dendrites of pyramidal cells (layer 2/3) in visual cortices of *Foxg1*$^{+/Cre}$ mice and wt littermates. As indicated in Fig. 6, no differences was present in spine length between the two genotypes (Fig. 6C) but a significant decrease in spine density was measured in *Foxg1*$^{+/Cre}$ as compared to wt mice (Fig. 6B). No difference was present in cell body diameter (wt N= 25 cells 16.9 µm SEM 2.3, *Foxg1*$^{+/Cre}$ N=24 cells 15.8 µm SEM 2.6; t-test p=0.76).

These results indicate that the severe impairment of visual acuity caused by Foxg1 haploinsufficiency is likely to be due to defects in the morphological organization of visual cortical neurons.

Discussion

In this report we demonstrate for the first time the functional consequences of *Foxg1* haploinsufficiency in the visual system of *Foxg1*$^{+/Cre}$ mice and a visual impairment in a cohort of Rett individuals presenting genetic alteration on *FOXG1*. Previous reports showed minor alterations in haploinsufficent animals consisting in a modestly thinner neocortex and reduced dentate gyrus size. To address this issue, we measured the visual acuity of *Foxg1*$^{+/Cre}$ mice and their wild type littermates by means of Visually Evoked Potentials (VEPs). Our results show that *Foxg1*$^{+/Cre}$ mice have a severe impairment in visual acuity and that the origin of such an impairment in visual function is not likely to reside in the retina, as retinal organization in these animals is normal. Indeed, retinal structure is qualitatively and quantitatively normal in *Foxg1*$^{+/Cre}$ mice, and previous work showed that loss of a single *Foxg1*allele does not impair development of retinofugal axons (Tian et al., 2008). Consistently with the animal model, all the examined subjects with *FOXG1* haploinsufficiency also show a visual impairment, with some common peculiarities. Such impairment seems to be principally caused by abnormal elaboration of visual signals in cortical areas.

Visual alterations in *FOXG1* mutated subjects

A common visual behavior reported in these subjects by relatives is the apparent lack of interest for any visual stimulus, often interpreted as low vision or narrowed visual field. This visual behavior

was better characterized in our subjects who mainly showed a scarce eye engagement, inconstant recognition of familial faces, and a general limited awareness to visual stimuli anywhere in the visual field, particularly when far and crowded. Despite a limited visual capacity, they were able to avoid obstacles and catch objects whenever positioned in neighboring space. The loss of attention and awareness for visual stimuli associated with the inability to disambiguate crowded objects or complex shapes; the inability of immediate recognition of familial faces, but the preserved interest and correct reaching or grasping toward colored stimuli and moving objects might suggest a condition resembling "blindsight". Blindsight syndrome is a well-recognized neuro-ophthalmological defect, which occurs upon extensive damage of the primary visual cortex (V1). Blindsight refers to the ability of cortically blind patients (bearing a primary visual cortex damage) to use extra striate visual information in guiding behaviors but in the absence of conscious object identification (Weiskrantz, 2009). Human blind-sight subjects are able to orient to and even answer questions about stimuli presented to the blind visual field. However, they are entirely unaware of the stimuli to which they are responding. Another characteristic of blindsight is that subjects can discriminate simple objects on the basis of their spatial frequency, shape, texture and color (Dineen and Keating, 1981), but they have lost the ability to identify more elaborate visual attributes, such as the capacity to visually recognize complex shapes or crowded objects, foods and familial faces. Moreover, blindsight patients well maintain reflexive saccades and motion perception, suggestingthat a residual network elaborating some visual information remains active even in case of extensive striate cortex lesions. The latter supports visually guided behaviors in the absence of awareness for visual stimuli. At least two separate pathways, and namely the retino-collicular and retino-geniculate pathways, reach the extrastriate cortex independently from the primary visual cortex, projecting to themotion area V5/MT in the medial temporal lobe. These connectionsmay represent theunconscious part of the dorsal 'where' visual stream, whereas the consciouscounterpart passes through the primary visual cortex before reachingthe V5/MT area. The extrastriate blind-sight pathways could be active in the *FOXG1* patients studied here, who indeed are attracted by colored and moving targets. On the contrary, their scarce awareness to visual stimuli might indicate a functional impairment of the striate visual pathway in the absence of retino-geniculate dysfunctions. This hypothesis (although not sustained by the demonstration of a structural damage of the occipital lobe detected by MRI) would suggest a functional impairment or incomplete maturation of the striate cortex as reinforced by the present results in the murine model.

Another visual system change in the human subjects studied here is the occurrence of ocular malformations, such as strabismus, oculo-mandibular syncinesias and small optic discs. These anomalies (observed in three individuals), together with other cerebral malformations (i.e. corpus

callosum hypoplasia) may represent the expression of a global immaturity of the brain due to *FOXG1* mutations.

Cortical architecture is defective in *Foxg1*$^{+/Cre}$ mice

Retinal structure appeared normal in *Foxg1*$^{+/Cre}$ mice, with no apparent anomalies in cell type distribution, laminar organization and numerical deficit in GCs that could explain the visual abnormalities. On the contrary, morphological studies showed significant changes in NeuN, PV and CR positive cells distribution in the visual cortex of *Foxg1*$^{+/Cre}$ mice compared to wild type animals. PV and CR are calcium binding proteins that serve as calcium buffers and label main subpopulations of GABA-ergic cortical interneurons. PV immunoreactivity develops postnatally: in mice, it appears around eye opening at P13-P14 in intermediate layers, from which it expands to the upper and inner cortical layers at subsequent developmental stages. In the visual cortex, PV positive cell maturation occurs during the critical period of ocular dominance plasticity and manipulations that accelerate or delay the time course of the critical period correspondingly regulate developmental maturation of PV cells. The decrease in PV cell density in uppermost layers and the increase in CR positive cells of *Foxg1*$^{+/Cre}$cortex suggest that Foxg1 haploinsufficiency results in an impairment in inhibitory circuitry maturation. PV+ synapses are usually perisomatic and PV+ pattern of innervation of pyramidal cells is engaged in controlof the spiking pattern. Their reciprocal and extensive connections can regulate the timing of activity in the cortex. Hence, we can speculate that the epileptic phenotype observed in *FOXG1* mutated patients (Brunetti-Pierri et al., 2011, Guerrini and Parrini, 2012) may be linked to a defective PV positive cells maturation. Conversely, CR positive cells usually synapse on dendrites; thus, the observed increase in CR positive cells in the lower layers of the *Foxg1*$^{+/Cre}$ cortex may cause a local alteration in cortical inhibition. Intriguingly, analysis of GAD67 positive neurons showed that the total number of inhibitory cells is preserved in *Foxg1*$^{+/Cre}$ mice. Thus, the reduction of NeuN positive neurons in the superficial layers is likely due to alterations of excitatory cells.

To further analyze the excitatory phenotype in *Foxg1*$^{+/Cre}$ primary visual cortex, we evaluated dendritic spine density and length in layer 2/3 pyramidal neurons. In the cerebral cortex, more than 90% of excitatory synapses terminate on spines. Spine density in the mouse neocortex increases during the second and third week of life and is followed by a period of major spine pruning and loss. In the primary visual cortex, dendritic spine density and morphology are developmentally regulated: they are plastic during young ages and become remarkably stable in adulthood. Our

results demonstrate a decrease in spine density in *Foxg1*$^{+/Cre}$ primary visual cortex compared to wild type animals.

Altogether, these results suggest that *Foxg1* haploinsufficiency causes alterations in both inhibitory and excitatory cells. Interestingly, alterations in inhibitory and excitatory synapses have been described in other mouse models of RTT as well as in a human disease model (iPSCs) obtained by genetic reprogramming of *FOXG1*-mutated patient fibroblasts (Patriarchi et al., 2015). In *MeCP2-KO* animals, the cortical excitatory input is reduced whilst the total inhibitory input is enhanced, leading to a shift of the homeostatic balance between excitation and inhibition in favor of inhibition. Moreover, MeCP2-deficient cortical and hippocampal neurons have fewer dendritic spines. *CDKL5*, the other gene found mutated in some cases of RTT, codes for a protein that has been demonstrated to localize at excitatory synapses, where it contributes to correct dendritic spine structure and synapse activity. *CDKL5* knockdown in cultured hippocampal neurons results in aberrant spine morphology (Chen et al., 2010) and unstable dendritic spines (Della Sala et al., 2015). Intriguingly, the analysis of novel mouse models carrying *Cdkl5* deletion showed alterations in sensory evoked potentials both in the auditory and the visual cortices (Wang et al., 2012, Amendola et al., 2014).

In conclusion, *Foxg1*haploinsufficiency causes a severe impairment in visual function that is likely due to altered cortical mechanisms. This should be taken into account when *Foxg1*$^{+/Cre}$ mice are used in behavioral experiments and when visual function is evaluated in patients carrying *FOXG1* mutations.

Acknowledgments

The work was partially funded by Telethon grant (GGP09117) and by Italian Health Ministry "Ricerca finalizzata 2010" (RF-2010-2317597) grant to AR. ES is recipient of a grant from Macula Vision Research Foundation.

References

Amendola E, Zhan Y, Mattucci C, Castroflorio E, Calcagno E, Fuchs C, Lonetti G, Silingardi D, Vyssotski AL, Farley D, Ciani E, Pizzorusso T, Giustetto M, Gross CT (Mapping pathological phenotypes in a mouse model of CDKL5 disorder. PLoS One 9:e91613.2014).

Ariani F, Hayek G, Rondinella D, Artuso R, Mencarelli MA, Spanhol-Rosseto A, Pollazzon M, Buoni S, Spiga O, Ricciardi S, Meloni I, Longo I, Mari F, Broccoli V, Zappella M, Renieri A (FOXG1 is responsible for the congenital variant of Rett syndrome. American journal of human genetics 83:89-93.2008).

Bahi-Buisson N, Nectoux J, Girard B, Van Esch H, De Ravel T, Boddaert N, Plouin P, Rio M, Fichou Y, Chelly J, Bienvenu T (Revisiting the phenotype associated with FOXG1 mutations: two novel cases of congenital Rett variant. Neurogenetics 11:241-249.2010).
Barone I, Novelli E, Piano I, Gargini C, Strettoi E (Environmental enrichment extends photoreceptor survival and visual function in a mouse model of retinitis pigmentosa. PLoS One 7:e50726.2012).
Belichenko PV, Wright EE, Belichenko NP, Masliah E, Li HH, Mobley WC, Francke U (Widespread changes in dendritic and axonal morphology in Mecp2-mutant mouse models of Rett syndrome: evidence for disruption of neuronal networks. J Comp Neurol 514:240-258.2009).
Brunetti-Pierri N, Paciorkowski AR, Ciccone R, Della Mina E, Bonaglia MC, Borgatti R, Schaaf CP, Sutton VR, Xia Z, Jelluma N, Ruivenkamp C, Bertrand M, de Ravel TJ, Jayakar P, Belli S, Rocchetti K, Pantaleoni C, D'Arrigo S, Hughes J, Cheung SW, Zuffardi O, Stankiewicz P (Duplications of FOXG1 in 14q12 are associated with developmental epilepsy, mental retardation, and severe speech impairment. Eur J Hum Genet 19:102-107.2011).
Castano G, Lyons CJ, Jan JE, Connolly M (Cortical visual impairment in children with infantile spasms. J AAPOS 4:175-178.2000).
Celesia GG (Steady-state and transient visual evoked potentials in clinical practice. Annals of the New York Academy of Sciences 388:290-307.1982).
Chen Q, Zhu YC, Yu J, Miao S, Zheng J, Xu L, Zhou Y, Li D, Zhang C, Tao J, Xiong ZQ (CDKL5, a protein associated with rett syndrome, regulates neuronal morphogenesis via Rac1 signaling. J Neurosci 30:12777-12786.2010).
Damiani D, Novelli E, Mazzoni F, Strettoi E (Undersized dendritic arborizations in retinal ganglion cells of the rd1 mutant mouse: a paradigm of early onset photoreceptor degeneration. J Comp Neurol 520:1406-1423.2012).
Dani VS, Chang Q, Maffei A, Turrigiano GG, Jaenisch R, Nelson SB (Reduced cortical activity due to a shift in the balance between excitation and inhibition in a mouse model of Rett syndrome. Proc Natl Acad Sci U S A 102:12560-12565.2005).
Dastidar SG, Bardai FH, Ma C, Price V, Rawat V, Verma P, Narayanan V, D'Mello SR (Isoform-specific toxicity of Mecp2 in postmitotic neurons: suppression of neurotoxicity by FoxG1. The Journal of neuroscience : the official journal of the Society for Neuroscience 32:2846-2855.2012).
De Filippis R, Pancrazi L, Bjorgo K, Rosseto A, Kleefstra T, Grillo E, Panighini A, Cardarelli F, Meloni I, Ariani F, Mencarelli MA, Hayek J, Renieri A, Costa M, Mari F (Expanding the phenotype associated with FOXG1 mutations and in vivo FoxG1 chromatin-binding dynamics. Clin Genet 82:395-403.2012).
de Freitas Dotto P, Cavascan NN, Berezovsky A, Sacai PY, Rocha DM, Pereira JM, Salomao SR (Sweep visually evoked potentials and visual findings in children with West syndrome. Eur J Paediatr Neurol 18:201-210.2014).
Della Sala G, Putignano E, Chelini G, Melani R, Calcagno E, Michele Ratto G, Amendola E, Gross CT, Giustetto M, Pizzorusso T (Dendritic Spine Instability in a Mouse Model of CDKL5 Disorder Is Rescued by Insulin-like Growth Factor 1. Biological psychiatry.2015).
Dineen J, Keating EG (The primate visual system after bilateral removal of striate cortex. Survival of complex pattern vision. Exp Brain Res 41:338-345.1981).
Duggan CD, DeMaria S, Baudhuin A, Stafford D, Ngai J (Foxg1 is required for development of the vertebrate olfactory system. J Neurosci 28:5229-5239.2008).
Durand S, Patrizi A, Quast KB, Hachigian L, Pavlyuk R, Saxena A, Carninci P, Hensch TK, Fagiolini M (NMDA receptor regulation prevents regression of visual cortical function in the absence of Mecp2. Neuron 76:1078-1090.2012).

Eagleson KL, Schlueter McFadyen-Ketchum LJ, Ahrens ET, Mills PH, Does MD, Nickols J, Levitt P (Disruption of Foxg1 expression by knock-in of cre recombinase: effects on the development of the mouse telencephalon. Neuroscience 148:385-399.2007).
Fiala JC, Spacek J, Harris KM (Dendritic spine pathology: cause or consequence of neurological disorders? Brain Res Brain Res Rev 39:29-54.2002).
Gan WB, Grutzendler J, Wong WT, Wong RO, Lichtman JW (Multicolor "DiOlistic" labeling of the nervous system using lipophilic dye combinations. Neuron 27:219-225.2000).
Guerrini R, Parrini E (Epilepsy in Rett syndrome, and CDKL5- and FOXG1-gene-related encephalopathies. Epilepsia 53:2067-2078.2012).
Hebert JM, McConnell SK (Targeting of cre to the Foxg1 (BF-1) locus mediates loxP recombination in the telencephalon and other developing head structures. Developmental biology 222:296-306.2000).
Jeon CJ, Strettoi E, Masland RH (The major cell populations of the mouse retina. J Neurosci 18:8936-8946.1998).
Krishnan K, Wang BS, Lu J, Wang L, Maffei A, Cang J, Huang ZJ (MeCP2 regulates the timing of critical period plasticity that shapes functional connectivity in primary visual cortex. Proceedings of the National Academy of Sciences of the United States of America 112:E4782-4791.2015).
Landi S, Putignano E, Boggio EM, Giustetto M, Pizzorusso T, Ratto GM (The short-time structural plasticity of dendritic spines is altered in a model of Rett syndrome. Sci Rep 1:45.2011).
Le Guen T, Bahi-Buisson N, Nectoux J, Boddaert N, Fichou Y, Diebold B, Desguerre I, Raqbi F, Daire VC, Chelly J, Bienvenu T (A FOXG1 mutation in a boy with congenital variant of Rett syndrome. Neurogenetics 12:1-8.2011a).
Le Guen T, Fichou Y, Nectoux J, Bahi-Buisson N, Rivier F, Boddaert N, Diebold B, Heron D, Chelly J, Bienvenu T (A missense mutation within the fork-head domain of the forkhead box G1 Gene (FOXG1) affects its nuclear localization. Hum Mutat 32:E2026-2035.2011b).
LeBlanc JJ, DeGregorio G, Centofante E, Vogel-Farley VK, Barnes K, Kaufmann WE, Fagiolini M, Nelson CA (Visual evoked potentials detect cortical processing deficits in Rett syndrome. Ann Neurol 78:775-786.2015).
Lenassi E, Likar K, Stirn-Kranjc B, Brecelj J (VEP maturation and visual acuity in infants and preschool children. Doc Ophthalmol 117:111-120.2008).
Lonetti G, Angelucci A, Morando L, Boggio EM, Giustetto M, Pizzorusso T (Early environmental enrichment moderates the behavioral and synaptic phenotype of MeCP2 null mice. Biol Psychiatry 67:657-665.2010).
Mariani J, Coppola G, Zhang P, Abyzov A, Provini L, Tomasini L, Amenduni M, Szekely A, Palejev D, Wilson M, Gerstein M, Grigorenko EL, Chawarska K, Pelphrey KA, Howe JR, Vaccarino FM (FOXG1-Dependent Dysregulation of GABA/Glutamate Neuron Differentiation in Autism Spectrum Disorders. Cell 162:375-390.2015).
Mencarelli MA, Spanhol-Rosseto A, Artuso R, Rondinella D, De Filippis R, Bahi-Buisson N, Nectoux J, Rubinsztajn R, Bienvenu T, Moncla A, Chabrol B, Villard L, Krumina Z, Armstrong J, Roche A, Pineda M, Gak E, Mari F, Ariani F, Renieri A (Novel FOXG1 mutations associated with the congenital variant of Rett syndrome. J Med Genet 47:49-53.2010).
Pancrazi L, Di Benedetto G, Colombaioni L, Della Sala G, Testa G, Olimpico F, Reyes A, Zeviani M, Pozzan T, Costa M (Foxg1 localizes to mitochondria and coordinates cell differentiation and bioenergetics. Proc Natl Acad Sci U S A 112:13910-13915.2015).
Patriarchi T, Amabile S, Frullanti E, Landucci E, Lo Rizzo C, Ariani F, Costa M, Olimpico F, J WH, F MV, Renieri A, Meloni I (Imbalance of excitatory/inhibitory synaptic protein expression in iPSC-derived neurons from FOXG1 patients and in foxg1 mice. Eur J Hum Genet.2015).

Pauley S, Lai E, Fritzsch B (Foxg1 is required for morphogenesis and histogenesis of the mammalian inner ear. Dev Dyn 235:2470-2482.2006).
Philippe C, Amsallem D, Francannet C, Lambert L, Saunier A, Verneau F, Jonveaux P (Phenotypic variability in Rett syndrome associated with FOXG1 mutations in females. J Med Genet 47:59-65.2010).
Porciatti V, Pizzorusso T, Maffei L (The visual physiology of the wild type mouse determined with pattern VEPs. Vision Res 39:3071-3081.1999).
Pratt T, Tian NM, Simpson TI, Mason JO, Price DJ (The winged helix transcription factor Foxg1 facilitates retinal ganglion cell axon crossing of the ventral midline in the mouse. Development 131:3773-3784.2004).
Rodriguez AR, de Sevilla Muller LP, Brecha NC (The RNA binding protein RBPMS is a selective marker of ganglion cells in the mammalian retina. The Journal of comparative neurology 522:1411-1443.2014).
Shen L, Nam HS, Song P, Moore H, Anderson SA (FoxG1 haploinsufficiency results in impaired neurogenesis in the postnatal hippocampus and contextual memory deficits. Hippocampus 16:875-890.2006).
Shoichet SA, Kunde SA, Viertel P, Schell-Apacik C, von Voss H, Tommerup N, Ropers HH, Kalscheuer VM (Haploinsufficiency of novel FOXG1B variants in a patient with severe mental retardation, brain malformations and microcephaly. Hum Genet 117:536-544.2005).
Siegenthaler JA, Tremper-Wells BA, Miller MW (Foxg1 haploinsufficiency reduces the population of cortical intermediate progenitor cells: effect of increased p21 expression. Cereb Cortex 18:1865-1875.2008).
Striano P, Paravidino R, Sicca F, Chiurazzi P, Gimelli S, Coppola A, Robbiano A, Traverso M, Pintaudi M, Giovannini S, Operto F, Vigliano P, Granata T, Coppola G, Romeo A, Specchio N, Giordano L, Osborne LR, Gimelli G, Minetti C, Zara F (West syndrome associated with 14q12 duplications harboring FOXG1. Neurology 76:1600-1602.2011).
Tian NM, Pratt T, Price DJ (Foxg1 regulates retinal axon pathfinding by repressing an ipsilateral program in nasal retina and by causing optic chiasm cells to exert a net axonal growth-promoting activity. Development 135:4081-4089.2008).
Tohyama J, Yamamoto T, Hosoki K, Nagasaki K, Akasaka N, Ohashi T, Kobayashi Y, Saitoh S (West syndrome associated with mosaic duplication of FOXG1 in a patient with maternal uniparental disomy of chromosome 14. Am J Med Genet A 155A:2584-2588.2011).
tom Dieck S, Brandstatter JH (Ribbon synapses of the retina. Cell and tissue research 326:339-346.2006).
Tomassy GS, Morello N, Calcagno E, Giustetto M (Developmental abnormalities of cortical interneurons precede symptoms onset in a mouse model of Rett syndrome. Journal of neurochemistry 131:115-127.2014).
Tropea D, Van Wart A, Sur M (Molecular mechanisms of experience-dependent plasticity in visual cortex. Philosophical transactions of the Royal Society of London Series B, Biological sciences 364:341-355.2009).
Wang IT, Allen M, Goffin D, Zhu X, Fairless AH, Brodkin ES, Siegel SJ, Marsh ED, Blendy JA, Zhou Z (Loss of CDKL5 disrupts kinome profile and event-related potentials leading to autistic-like phenotypes in mice. Proc Natl Acad Sci U S A 109:21516-21521.2012).
Wassle H, Puller C, Muller F, Haverkamp S (Cone contacts, mosaics, and territories of bipolar cells in the mouse retina. J Neurosci 29:106-117.2009).
Weiskrantz L (Is blindsight just degraded normal vision? Exp Brain Res 192:413-416.2009).
Williams RW, Strom RC, Goldowitz D (Natural variation in neuron number in mice is linked to a major quantitative trait locus on Chr 11. The Journal of neuroscience : the official journal of the Society for Neuroscience 18:138-146.1998).
Xiang M, Zhou L, Peng YW, Eddy RL, Shows TB, Nathans J (Brn-3b: a POU domain gene expressed in a subset of retinal ganglion cells. Neuron 11:689-701.1993).

Xuan S, Baptista CA, Balas G, Tao W, Soares VC, Lai E (Winged helix transcription factor BF-1 is essential for the development of the cerebral hemispheres. Neuron 14:1141-1152.1995).

The authors wish it to be known that, in their opinion, the first two authors should be regarded as joint First Authors.

Legend to Figures

Figure 1. Visual acuity in *Foxg1*$^{+/Cre}$ mice and wild-type littermates

(*A*) Examples of VEP waveforms recorded in response to 0.1 c/deg gratings. *(B)* VEP amplitude changes in response to gratings of high contrast and of decreasing bar size (increasing spatial frequency) in a wild-type (WT) and a *Foxg1*$^{+/Cre}$ mouse. VEP amplitude decreases by progressively increasing the spatial frequency. Visual acuity was determined by linearly extrapolating VEP amplitude to 0 V. Symbols represent data average data from all animals (WT n=9; *Foxg1*$^{+/Cre}$ *n*=5). Arrows in the abscissa point to visual acuity value. Dotted line represents average noise level. *(C)* Spatial resolution in the visual cortex of wild-type and *Foxg1*$^{+/Cre}$mice. Visual acuity is significantly reduced in *Foxg1*$^{+/Cre}$mice compared with wild-type littermates (*Foxg1*$^{+/Cre}$, 0.20 cycle/degree SEM 0.05, n=9; WT, 0.51 cycle/degree, SEM 0.05 n=5; *****, *P*,0.01, Student's *t* test).

Figure 2. Retinal morphology in *Foxg1*$^{+/Cre}$ animals and wild-type littermates

Retinal morphology in *Foxg1*$^{+/Cre}$ (A and C) and wt (B and D) mice. A, B: Low magnification images of retinal sections stained with rhodopsin antibodies (green signal), showing normal retinal laminations and bright staining of photoreceptor outer segments (OS) in both mutant and wt mice. Red: nuclear counterstaining. In A the normal morphology of the optic nerve head (ONH) can be appreciated. The insets show at 2x details of photoreceptor rows and outer segments. Here and in the following images: ONL, IPL outer nuclear and inner plexiform layer, respectively. C and D: examples of retinal ganglion cells (GC) stained by the type specific transcription factor Brn3-B (red), with nuclear localization, and by neurofilament antibodies (green), depicting their morphology in detail.

Figure 3. M**orphology of neuronal subtypes in *Foxg1*$^{+/Cre}$ mice and wild-type littermates**

Morphology of retinal neuronal subtypes in *Foxg1*$^{+/Cre}$ (left panels) and wt mice

Retinal neurons in *Foxg1*$^{+/Cre}$ (left panels) and wt mice. A, B: rod bipolar cells have been labelled red by PKC antibodies. Their dendrites form dense plexa in the OPL while axonal endings (rbe) cluster in regularly in the deepest part of the IPL. Green puncta are synaptic ribbons from glutamatergic processes, regularly arranged in the two plexiform layers. Blue: nuclearcounterstaining. C,D: types of cone bipolar cells stained by ZnP-1 (synaptotagmin antibodies). Both dendritic tips in the OPL and axonal arbors in the IPL have the expected fine structure. The IPL show three typical bands, revealed by calretinin staining of amacrine cells (red). E, F: Cholinergic amacrine cells, stained red by ChAT antibodies, are arranged in two mirror-

symmetric populations at the two margins of the IPL. Alpha-like ganglion cells, labelled by SMI-32 antibodies (green) have well preserved morphologies in both mutant and wt retinas.

Fig.4. Neurons in the GCL of *Foxg1*$^{+/+}$ and *Foxg1*$^{+/Cre}$ mice

A,B. Cells in the GCL have been labelled by antibodies against the RNA binding protein RBPMS that produce a cytoplasmic staining in GCs selectively (green signal). Ethidium counterstaining (red signal) show the nuclei of GCs and displaced amacrine cells (AC).The general morphology (A and B) and the total number of cells in the GC layer (C) are virtually identical in *Foxg1*$^{+/+}$ (A) and *Foxg1*$^{+/Cre}$ (B) mice. Quantification in C. The number of GCs proper (D) is also not different between the two strains (D).

Figure 5. Immunohistochemistry on visual cortex of *Foxg1*$^{+/+}$ and *Foxg1*$^{+/Cre}$ mice

Panel A. A significant reduction of NeuN staining is present in layer II-III and IV of the visual cortex of Foxg1$^{+/Cre}$ mice (WT: n=4; *Foxg1*$^{+/Cre}$= n=4; two-ways RM ANOVA genotype X cortical layer p=0.003; post-hoc Sidak wt vs. *Foxg1*$^{+/Cre}$ within layer II-III p=0.004, within layer IV p=0.006).

Panel B. Calretinin positive cells in visual cortices from WT and *Foxg1*$^{+/Cre}$ mice. Quantification of calretinin positive cells density in visual cortical layers of WT and *Foxg1*$^{+/Cre}$ mice shows a significant increase of calretinin positive cells in layer II-III and VI of the *Foxg1*$^{+/Cre}$ cortex (two-ways RM ANOVA genotype X cortical layer p=0.04; post-hoc Sidak wt vs. *Foxg1*$^{+/Cre}$ within layer II-III p<0.01, within layer VI p<0.05).

Panel C Parvalbumin positive cells in visual cortices from WT and *Foxg1*$^{+/Cre}$ mice. Quantification of parvalbumin positive cells density in visual cortical layers of WT and *Foxg1*$^{+/Cre}$ mice shows a significant decrease of parvalbumin positive cells in layer II-III of the *Foxg1*$^{+/Cre}$ cortex (two-ways RM ANOVA genotype X cortical layer p=0.03; post-hoc Sidak wt vs. *Foxg1*$^{+/Cre}$ within layer II-III p<0.01).

Panel D GAD67 positive cells in visual cortices from WT and *Foxg1*$^{+/Cre}$ mice. Quantification of GAD67 positive cells density in visual cortical layers of WT and *Foxg1*$^{+/Cre}$ mice shows that the density of GAD67 positive cells is not statistically different between wt and *Foxg1*$^{+/Cre}$ mice (two-ways RM ANOVA effect of genotype p=0.44, genotype X cortical layer p=0.33)..*: p<0.05; **: p<0.01.

Figure 6. Dendritic spine length and density in *Foxg1*$^{+/Cre}$ animals and wild-type littermates

A) Confocal microscope images of WT and *Foxg1*$^{+/Cre}$dendritic segment. Scale bar= 5µm. B and C) Average dendritic spine length and density (respectively) in basal dendrites of layer 4/5 pyramidal cells of *Foxg1*$^{+/Cre}$and WT mice. A significant decrease in spine density was measured in *Foxg1*$^{+/Cre}$ as compared to wt mice (WT: n= 7; *Foxg1*$^{+/Cre}$: n=7; p=0.045, Student's *t* test).

Figure 1

Click here to download Figure: fig 1.pptx

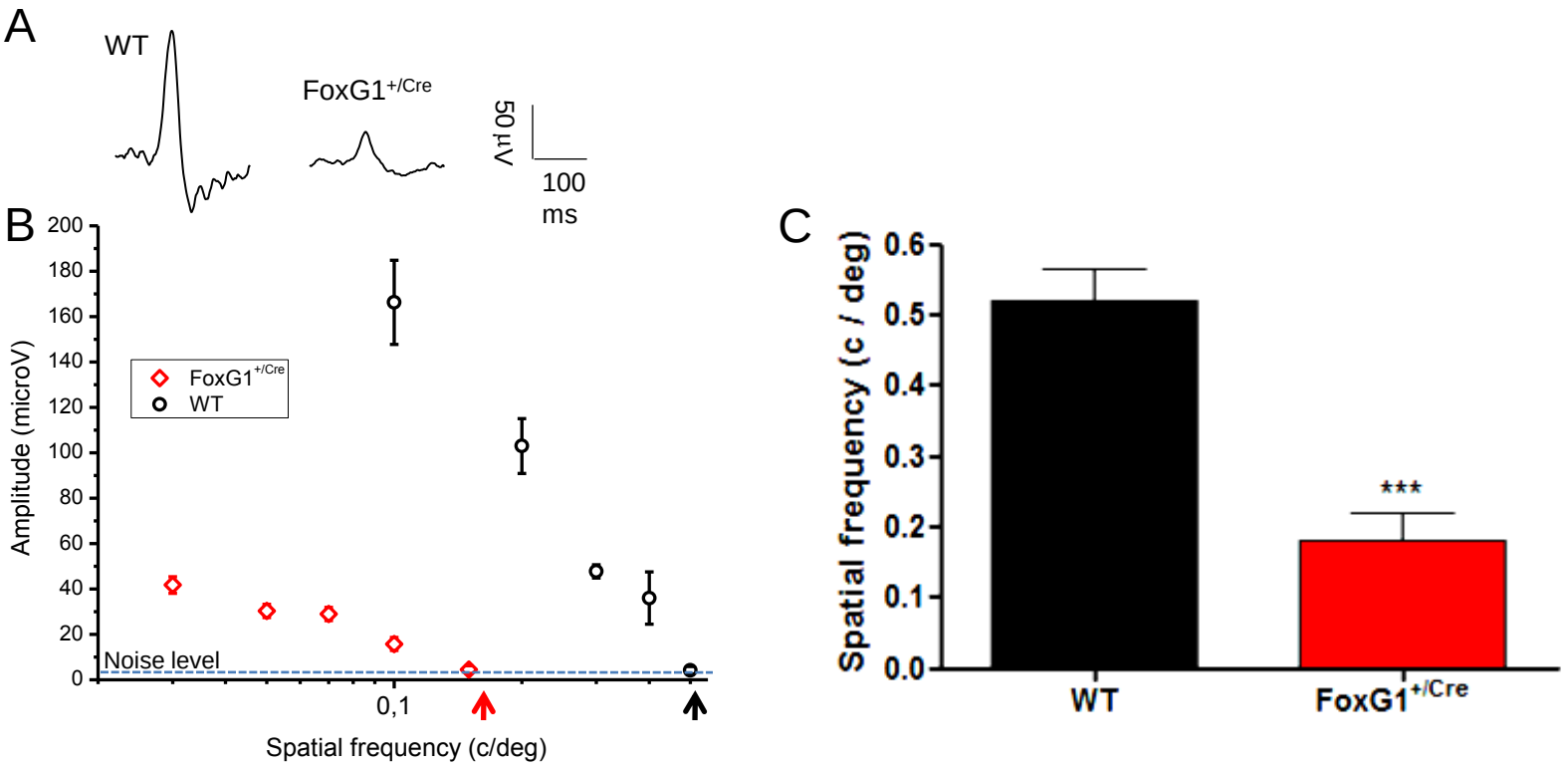

Fig. 1

Figure 2

Click here to download Figure: fig 2.pptx

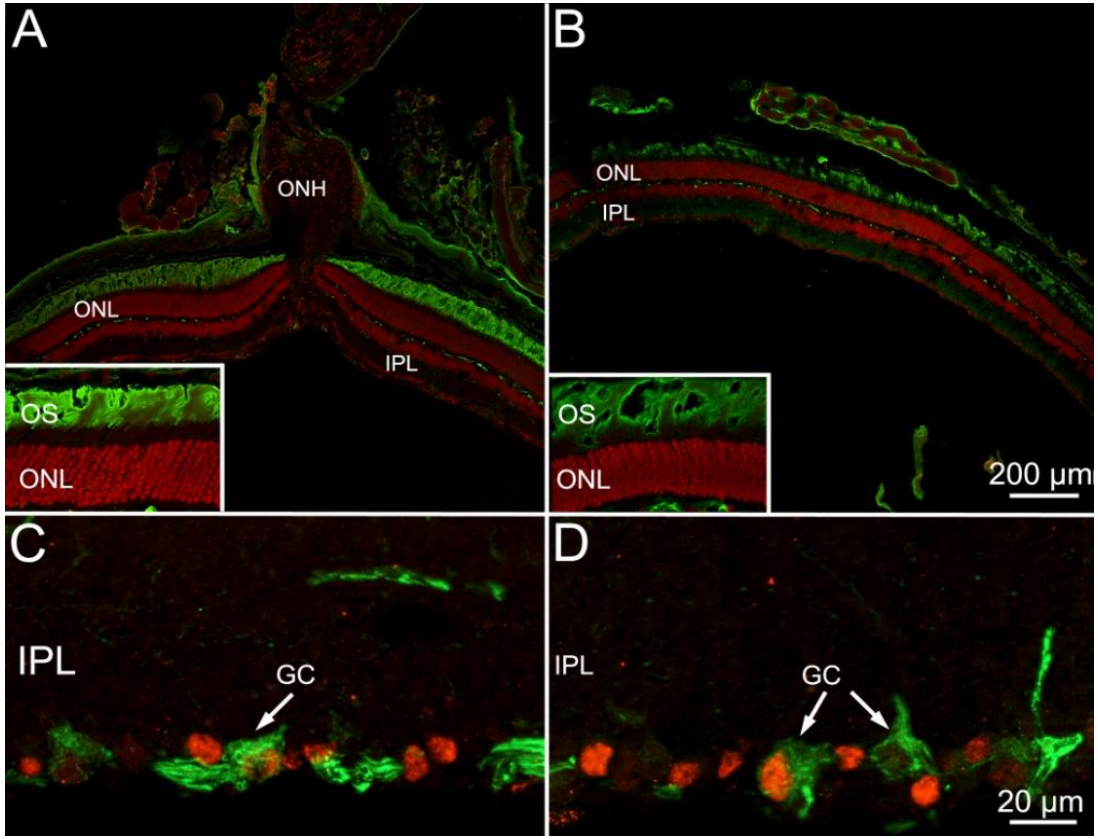

Fig. 2

Figure 3

Click here to download Figure: fig 3.pptx

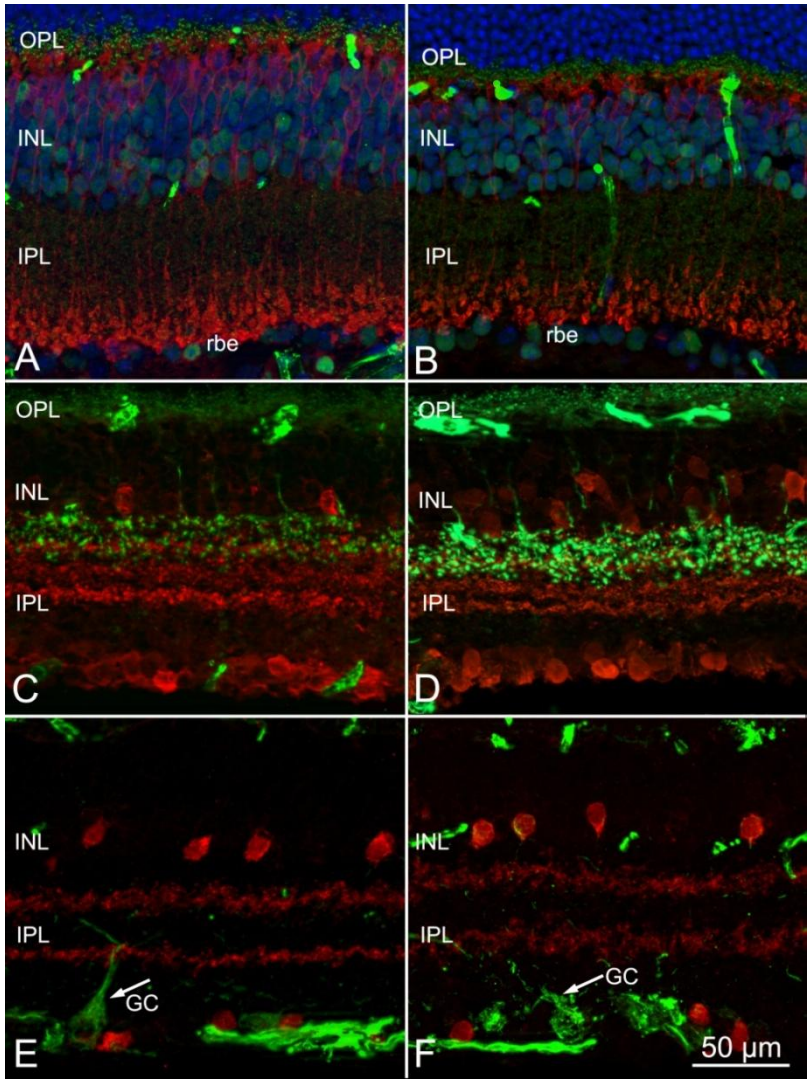

Fig.3

Figure 4

Click here to download Figure: fig 4.pptx

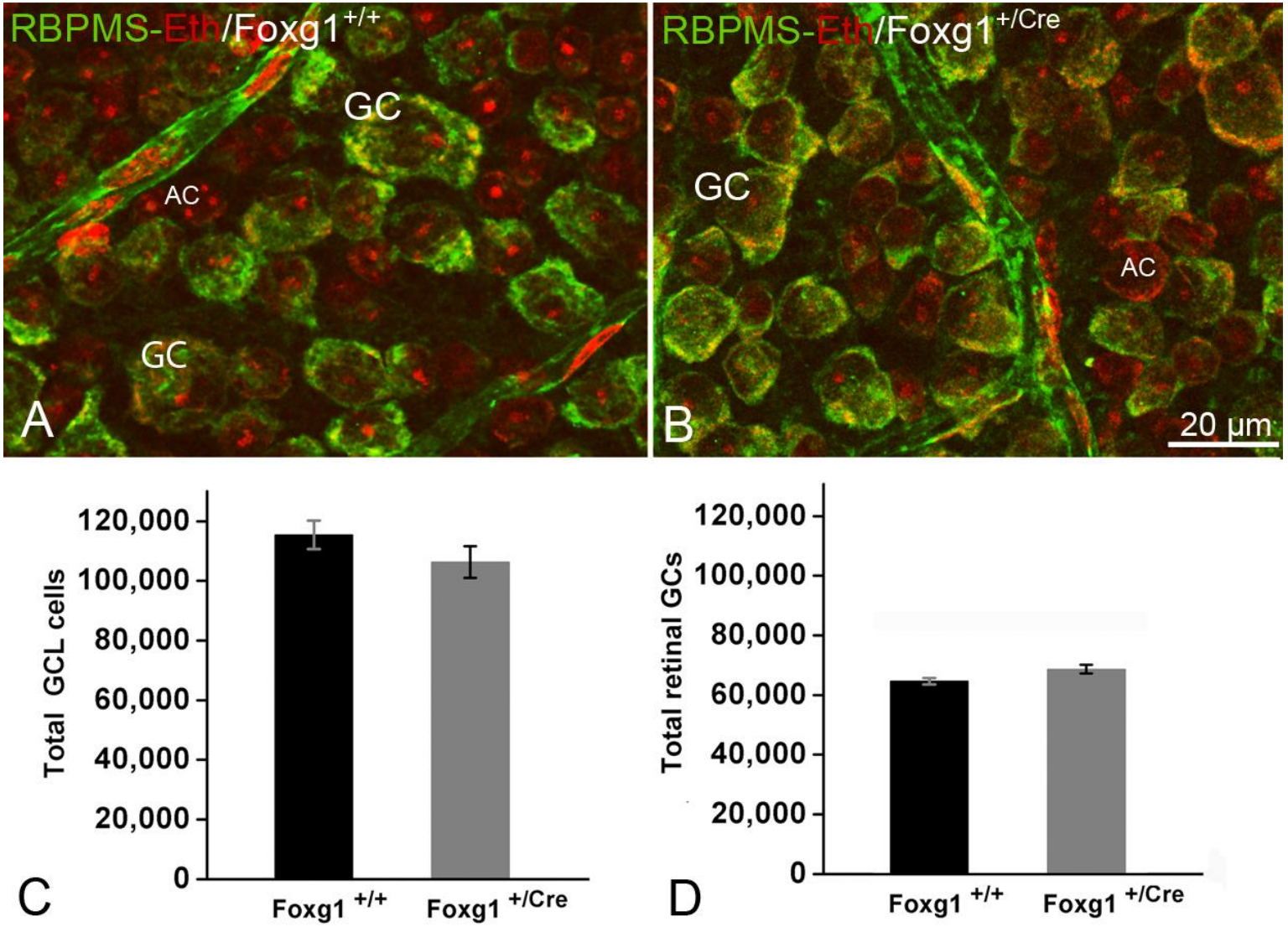

Fig. 4

Figure 5

Click here to download Figure: fig 5.pptx

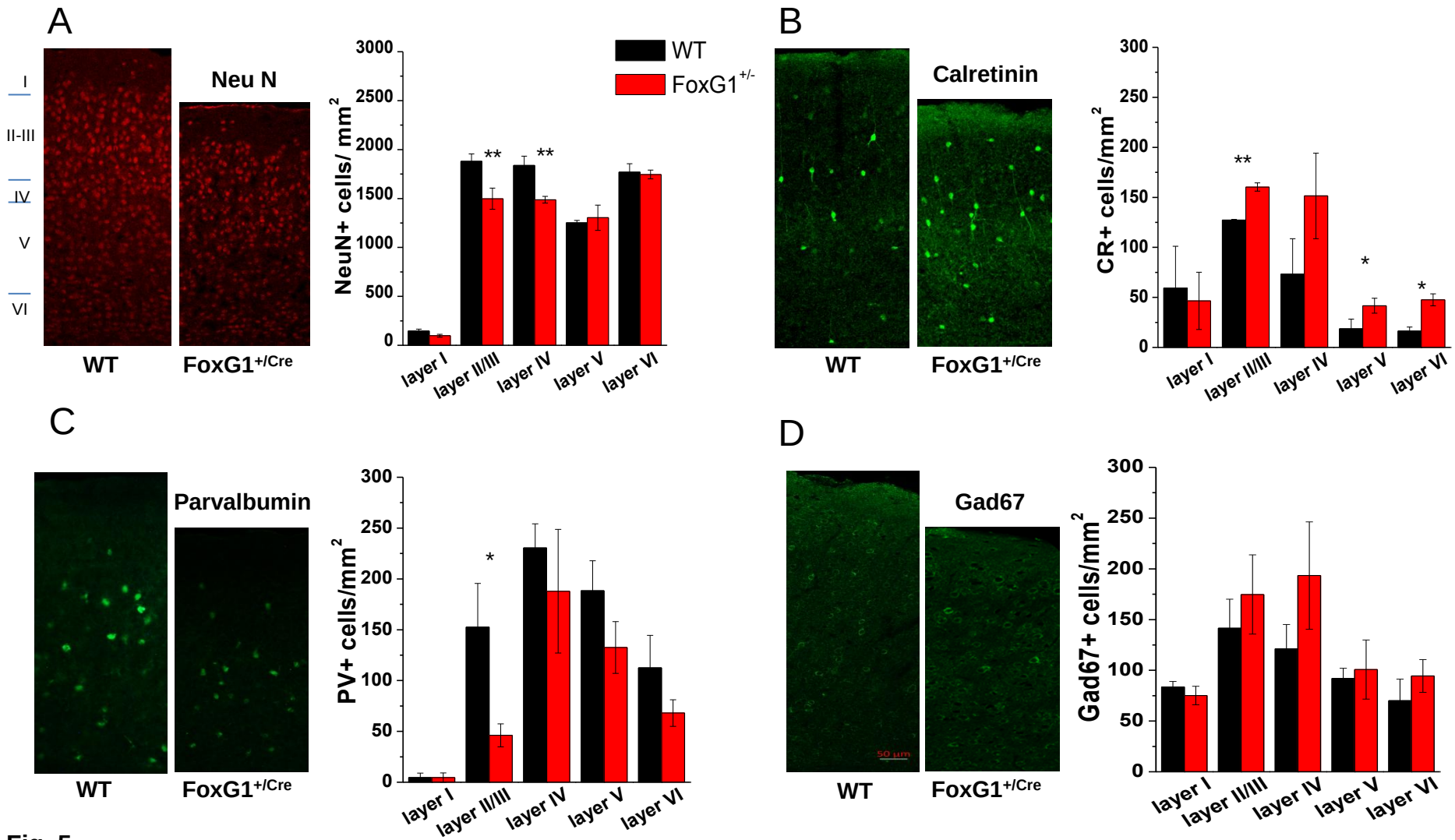

Fig. 5

Figure 6

Click here to download Figure: fig 6.pptx

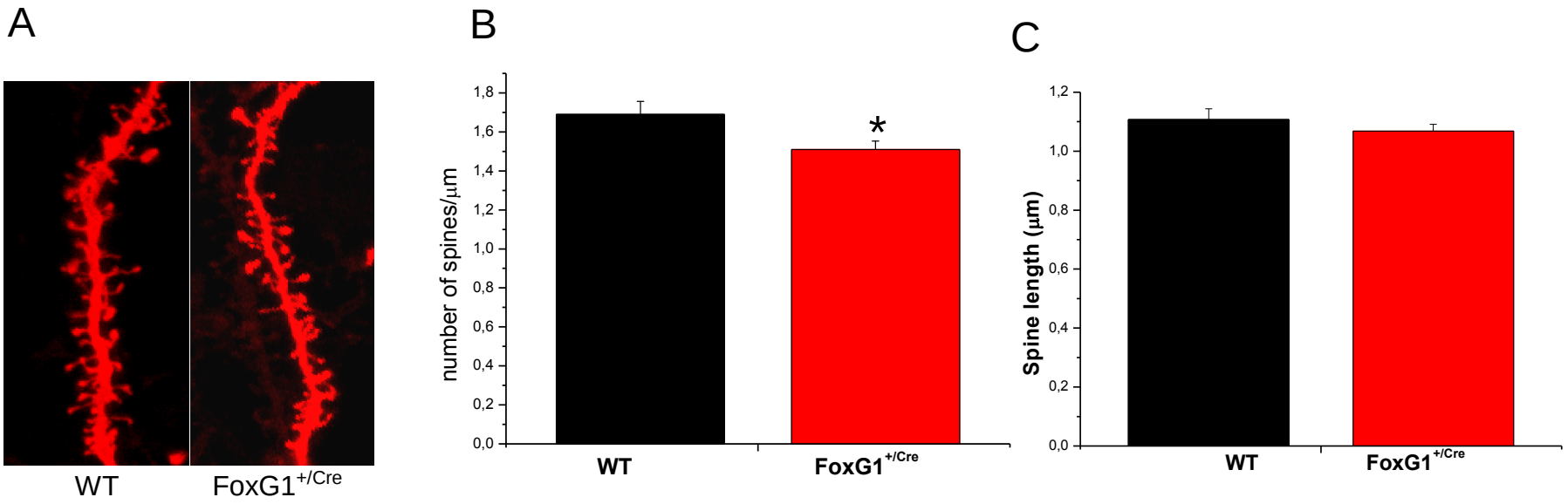

Fig.6

Table 1

Table 1. summary of patients features and clinical results

Patient	Sample ID	Sex	Age	*FOXG1* mutation	Attention and awareness to visual stimuli	Deficit to distinguish far stationary crowded objects	Familiar faces recognition	Diss. between looking and reaching	Absent or reduced visual contact	Colored visual stimuli awareness	Moving target vision	Fixation and engagement	Eye movement and alignment	Photophobia or compulsive gazing to the light	Fundoscopy	VEP flash	EEG	MRI
1	/	F	9m	6,73 Mb Del chr 14: 26,633,912-33,360,894	No	yes	Inconstant	yes	yes	NE	yes	scarce	Exotropia	No	small optic disks OD>OS	NE	NE	Corpus Callosum agenesis
2	/	M	1y 8m	c.762C>Gp. Tyr254*	No	yes	No	yes	yes	yes	Inconstant	scarce	Eexotropia Upbeating nystagmus	Yes	Small normal appearing optic nerves	NE	Occipital-Parietal activity	NE
3	#934/2013	F	2y 7m	6,37 Mb del chr 14: 26,908,842-33,280,997	No	yes	Inconstant	yes	yes	yes	yes	poor for distance sufficient for near	Esotropia, oculomandibular syncinesia	Yes	Normal	NE	Normal	Corpus Callosum agenesis, colpocephaly, subversion of hippocampus
4	#2362	F	3y 5m	1,1 Mb Del chr 14: 27,622,465-28,725,069	No	yes	No	yes	yes	yes	yes	scarce for distance better for near	Exotropia Ocualr apraxia	No	Normal	NE	NE	Corpus Callosum agenesis
5	/	M	5 y	c.651C>Gp. Y217X	No	yes	No	yes	yes	Yes	yes	poor	strabismus surgically treated	preference for bright light	small optic disk in OD	NE	NE	NE
6	#611/2013	F	1y 5m	c.460dupG, p.Glu154Glyfs*300	No	yes	Inconstant	yes	yes	Yes	yes	scarce	Exotropia	Yes	Normal	L: 102ms A: 9.7 µV	Normal	Corpus Callosum dysgenesis, mild symplified gyral pattern
7	#1009/2013	M	2y 5m	1.8 Mb Del chr 14: 28,339,878-30,108,071	No	yes	No	yes	yes	Yes	yes	good	Esotropia	Yes	Normal	L:104 ms A:7.7 µV	Generalized epilepsy	Normal
8^	#156	F	22y	c.756G>Ap. W255X	No	yes	Inconstant	yes	yes	NE	yes	scarce	Exotropia	No	Normal	L: 100 ms A:10 µV	Slowing in Occipital and Temporal regions	Corpus Callosum hypoplasia, hyporplasic hemispheres

NE: not evaluated
^This case corresponds to Patient 1 in Ariani et al (1)
L: Latency of the first positive inflection peak, normally close to 100 ms after stimulus onset (range between 90-105 ms in normal controls)
A: Amplitude of the main positive peak (N75-P100) after the stimulus onset, ranged between 5.3 to 10 µV in normal controls